bioRxiv preprint doi: https://doi.org/10.1101/2020.01.22.915397; this version posted January 23, 2020. The copyright holder for this preprint (which was not certified by peer review) is the author/funder, who has granted bioRxiv a license to display the preprint in perpetuity. It is made available under aCC-BY 4.0 International license.

Medical data and machine learning improve power of stroke genome-wide association studies

Phyllis M. Thangaraj[a,b,c], Nicholas P. Tatonetti[b,c,d,*]

[a]*Integrated Program in Cellular, Molecular, and Biomedical Studies, Columbia University Irving Medical Center, New York, NY*
[b]*Department of Systems Biology, Columbia University Irving Medical Center, New York, NY*
[c]*Department of Biomedical Informatics, Columbia University Irving Medical Center, New York, NY*
[d]*Department of Medicine, Columbia University Irving Medical Center, New York, NY*

Abstract

Genome-wide association studies (GWAS) may require enrollment of up to millions of participants to power variant discovery. This requires manual curation of cases and controls with large-scale collaborations. Biobanks connected to electronic health records (EHR) can facilitate these studies by using data from clinical care systems, like billing diagnosis codes, as phenotypes. These systems, however, do not define adjudicated cases and controls. Machine learning can add nuance to these definitions. We developed QTPhenProxy, a machine learning model that assigns everyone in a cohort a probability of having the study disease, and then run a GWAS using the probabilities as a quantitative trait. With an order of magnitude fewer cases than the largest stroke GWAS, our method outperformed previous methods at replicating known variants in stroke and discovered a novel variant in ABCG8 associated with intracerebral hemorrhage in the UK Biobank. QTPhenProxy expands traditional phenotyping to improve the power of GWAS.

*Corresponding Author
Email address: nick.tatonetti@columbia.edu (Nicholas P. Tatonetti)

bioRxiv preprint doi: https://doi.org/10.1101/2020.01.22.915397; this version posted January 23, 2020. The copyright holder for this preprint (which was not certified by peer review) is the author/funder, who has granted bioRxiv a license to display the preprint in perpetuity. It is made available under aCC-BY 4.0 International license.

Keywords:

electronic health records phenotyping, stroke, genome-wide association studies, machine learning

---

1. Introduction

Large genetic repositories connected to electronic health records (EHR) promise the ability to perform thousands of genetic studies using data routinely captured in clinical practice. High-throughput identification of cases and controls can be difficult, however, due to time-consuming chart review and incompleteness of medical records. Current disease genome-wide association studies develop case-control sets in which power relies on a large amount of pure cases, and the missingness of EHR data could prevent some cases from discovery in a high-throughput manner McCarthy et al. (2008); Weiskopf et al. (2013); DeBoever et al. (2019). In addition, extreme case-control imbalance in biobanks can lead to increased type 1 error when running linear mixed model genome-wide association analysis Zhou et al. (2018). An incorporation of additional accessible EHR data could improve case curation sensitivity. In addition, many diseases such as stroke result from a combination of gene and environmental interactions, and there is significant overlap with co-morbidities in genome-wide significant variants Malik et al. (2018a). Therefore, it is difficult to confirm every person without the event a control, suggesting the utility of a disease likelihood assignment McCarthy et al. (2008); Yang et al. (2009).

The definition of the disease phenotype influences the success of detecting a genetic signal since power is generally calculated by number of cases and controls Maher (2008); Zaykin and Zhivotovsky (2005). We propose that including EHR

bioRxiv preprint doi: https://doi.org/10.1101/2020.01.22.915397; this version posted January 23, 2020. The copyright holder for this preprint (which was not certified by peer review) is the author/funder, who has granted bioRxiv a license to display the preprint in perpetuity. It is made available under aCC-BY 4.0 International license.

information about comorbidities Kohane (2011) and other health information about our subject to trait assignment can improve the power of GWAS. Past studies have shown that incorporating diagnosis count improved the power of genetic studies, and the addition of patient questionnaires and genetic correlations to hospital records improved detection of cases Sinnott et al. (2018); DeBoever et al. (2019); Liu et al. (2017). We argue that including several modalities of health data to estimate assignment of case probability can improve the power of genomic studies. For example, the most successful genome-wide association study for stroke required 40,585 cases and 406,111 controls Malik et al. (2018a). We hypothesize that we can discover genome-wide significant variants associated with stroke with a fraction of those cases (4,354) by incorporating EHR information into a quantitative trait assignment.

In this study, we use machine learning methods to expand sample cohorts by assigning every patient a probability of disease. We hypothesize that the output of a supervised machine learning classifier, trained on the EHR data of a small number of known cases and controls, can be used as a proxy variable for stroke and will be an efficient strategy for expanding cohort size. We demonstrate that our quantitative proxy trait can improve power over its respective binary trait in ischemic stroke. We also show that the new variants discovered are known in similar cardiovascular and neurological diseases. We find up to 7 LD independent loci that pass genome-wide significance and conditional analysis, and the majority of the associated genes are known to be associated with stroke or cardiovascular disease. For stroke and its subtypes ischemic stroke, subarachnoid hemorrhage, and intracerebral hemorrhage, QTPhenProxy recovered known and discovered new stroke variants, such as in *ABCG8*, with an order of magnitude fewer cases

bioRxiv preprint doi: https://doi.org/10.1101/2020.01.22.915397; this version posted January 23, 2020. The copyright holder for this preprint (which was not certified by peer review) is the author/funder, who has granted bioRxiv a license to display the preprint in perpetuity. It is made available under aCC-BY 4.0 International license.

than traditional genome-wide association studies.

2. Results

2.1. QTPhenProxy has high model performance.

We trained models with 5 different classifier types and all stroke, ischemic stroke, intracerebral hemorrhage, and subarachnoid hemorrhage as defined by the UK Biobank Algorithmically Defined Outcomes rubric National Library of Medicine (b). Random forest models overall showed the best area under the receiver operating curve and adaboost models gave the best area under the precision recall curve on the hold-out test set (Supplementary Tables B.1 andB.3) . Overall stroke, followed by ischemic stroke showed high precision at top 50 patients ordered by probability (Figure 1, Table 1, Supplementary Table B.2). We chose the probabilities from the EN and RF models to run the genome-wide association analyses because the distribution of their probabilities was continuous and included values from 0-1 (Figure 1, Supplementary Figure A.1).

2.2. Novel and known variants are recovered by QTPhenProxy in higher numbers traditional binary method using the QC1 markers and principal components.

The binary trait logistic regression genome-wide association study for stroke, ischemic stroke, and subarachnoid hemorrhage recovered no variants with genome-wide significance. Binary trait logistic regression genome-wide association study for intracerebral hemorrhage recovered 2 variants with genome-wide significance. Quantitative trait linear regression using QTPhenProxy probabilities for stroke recovered 120 genome-wide significant SNPs with 16 LD-independent loci and 1215 genome-wide significant SNPs with 39 LD-independent loci, for ischemic

bioRxiv preprint doi: https://doi.org/10.1101/2020.01.22.915397; this version posted January 23, 2020. The copyright holder for this preprint (which was not certified by peer review) is the author/funder, who has granted bioRxiv a license to display the preprint in perpetuity. It is made available under aCC-BY 4.0 International license.

stroke recovered 202 genome-wide significant SNPs with 15 LD-independent loci, and 1266 genome-wide significant SNPs with 46 LD-independent loci, for subarachnoid hemorrhage recovered 69 genome-wide significant SNPs with 4 LD-independent loci, and 722 genome-wide significant SNPs with 40 LD-independent loci, and for intracerebral hemorrhage recovered 146 genome-wide significant SNPs with 8 LD-independent loci, and 1059 genome-wide significant SNPs with 54 LD-independent loci using the EN and RF classifiers, respectively (Table 1). We show the comparison of genome-wide significant variants between the QTPhenProxy EN model and Binary trait GWAS for stroke in a Hudson plot (Figure 2) Lucas. Out of known ischemic stroke variants, both models also recovered 3 known variants with genome-wide significance, and the EN model recovered 21/49 of the known variants, equivalent to a sensitivity of 0.428, while the traditional binary trait recovered 15/49, (sensitivity=0.306), and RF model recovered 14/49 (sensitivity=0.286) with nominal p-value of 0.05 (Table 1). For all stroke, sensitivity of known stroke variants was 0.333 using the EN model, 0.261 using the RF model, and 0.202 using the binary trait. Subarachnoid hemorrhage did not have a specific EBI-GWAS disease marker set, and the EBI-GWAS disease marker set for intracerebral hemorrhage only consisted of one variant. The difference in p-values between the binary and QTPhenProxy for known ischemic stroke variants was significantly increased compared to the same number of random variants using the EN classifier (two sample t test, t=2.43, p=0.0184 for EN classifier and t=1.74, p=0.0876 for RF classifier). In addition, QTPhenProxy with EN classifier showed a significant decrease in p-value of all known ischemic stroke variants compared to traditional binary method (two sample t-test, t=-2.1 p=0.0367) while QTPhenProxy with RF classifier did not show a significant decrease (t=-1.48,p=0.144).

bioRxiv preprint doi: https://doi.org/10.1101/2020.01.22.915397; this version posted January 23, 2020. The copyright holder for this preprint (which was not certified by peer review) is the author/funder, who has granted bioRxiv a license to display the preprint in perpetuity. It is made available under aCC-BY 4.0 International license.

The difference in p-values between the binary and QTPhenProxy for known all stroke variants was significantly increased compared to the same number of random variants for the EN classifier (t=2.80, p=0.00638) but not significant for the RF classifier (t=0.737,p=0.463). In addition, QTPhenProxy with EN classifier showed a decrease in p-value of all known stroke variants compared to traditional binary method (two sample t-test, t=-1.87 p=0.0639) while QTPhenProxy with RF classifier did not show a significant decrease (t=-1.05,p=0.298).

2.3. Novel and known variants are recovered by QTPhenProxy in higher numbers traditional binary method using the QC2 markers and principal components.

The binary trait logistic regression genome-wide association study for stroke, ischemic stroke, and subarachnoid hemorrhage recovered no variants with genome-wide significance. Binary trait logistic regression genome-wide association study for intracerebral hemorrhage recovered 2 variants with genome-wide significance. Quantitative trait linear regression using QTPhenProxy probabilities for stroke recovered 7 LD-independent loci, 3 LD-independent loci, for ischemic stroke, 3 LD-independent loci for subarachnoid hemorrhage, and 3 LD-independent loci for intracerebral hemorrhage using the EN classifier. We show the comparison of genome-wide significant variants between the EN and Binary in a Hudson plot (Figure 2) Lucas. Out of known ischemic stroke variants, both models also recovered 3 known variants with genome-wide significance, and the EN model recovered 16/49 of the known variants, equivalent to a sensitivity of 0.326, while the traditional binary trait recovered 15/49, (sensitivity=0.306), and RF model recovered 15/49 (sensitivity=0.306) with nominal p-value of 0.05 (Figure 3). For all stroke, sensitivity of known stroke variants was 0.265 using the EN model, 0.220 using the RF model, and 0.220 using the binary trait (Supplementary Figure

bioRxiv preprint doi: https://doi.org/10.1101/2020.01.22.915397; this version posted January 23, 2020. The copyright holder for this preprint (which was not certified by peer review) is the author/funder, who has granted bioRxiv a license to display the preprint in perpetuity. It is made available under aCC-BY 4.0 International license.

A.5). The t-tests referred to in 2.2 did not show significance.

2.4. Conditional analysis identifies novel variants with genome-wide significance using the QC1 markers and principal components.

Conditional analysis of the GWAS with QC1 quality control for the QTPhen-Proxy EN model for all stroke identified 13 candidate variants with genome-wide significance, all which are novel, though some of the nearest genes to these loci have been identified in previous studies through nearby loci. There were 12 loci identified for the stroke subtype ischemic stroke, 3 loci for subarachnoid hemorrhage, and 9 loci for intracerebral hemorrhage (Table 2). Several loci overlapped across stroke and some subtypes. Position 46705193 on chromosome 11, which is in an intronic section of *ARHGAP1* National Center for Biotechnology Information, National Library of Medicine., showed genome-wide significance in stroke, ischemic stroke, and intracerebral hemorrhage. A missense mutation at locus rs6025 in the *F5* gene showed genome-wide significance across stroke, intracerebral hemorrhage, and locus rs1894692, which is near the *F5* gene National Center for Biotechnology Information, National Library of Medicine., showed genome wide significance in ischemic stroke. Additional loci that showed genome-wide significance in both all stroke and ischemic stroke included those that are intronic to *LPA* and *NOS3* and nearby to *APOC1P1*/*APOC1* and *CDKN2A*/*CDKN2B* National Center for Biotechnology Information, National Library of Medicine.. Finally, all stroke and intracerebral hemorrhage shared additional loci that showed genome-wide significance after conditional analysis, which were nearby LOC105377992 and *RPS4X9* National Center for Biotechnology Information, National Library of Medicine.. All stroke genome-wide significant variants also included intronic loci in the *MTA3*, *SOX7*, *ABO*, *FURIN*, and *PLCB1* genes National Center for Biotech-

bioRxiv preprint doi: https://doi.org/10.1101/2020.01.22.915397; this version posted January 23, 2020. The copyright holder for this preprint (which was not certified by peer review) is the author/funder, who has granted bioRxiv a license to display the preprint in perpetuity. It is made available under aCC-BY 4.0 International license.

nology Information, National Library of Medicine.. Ischemic stroke genome-wide significant variants included intronic loci in the*LPAL2* gene, intergenic loci in the *PITX2*, *LDLR*, and an insertion mutation in the *ABO* gene National Center for Biotechnology Information, National Library of Medicine.. Subarachnoid hemorrhage genome-wide significant variants included an intronic locus in the *ABO* gene. Finally, intracerebral hemorrhage genome-wide significant variants included a missense mutation loci in the *ABCG8* gene, and intronic loci in the *NOS3* and *XKR6* genes National Center for Biotechnology Information, National Library of Medicine.. The variants near or in LOC105377992, *NOS3*, *CDKN2A*/*CDKN2B*, *LPA*, *LDLR*, *ABCG8*, and *RPS4X9* were below nominal significance of 0.05 in the MEGASTROKE stroke and ischemic stroke GWAS of European ancestry (Table 3) Malik et al. (2018a).

2.5. Conditional analysis identifies novel variants with genome-wide significance using the QC2 markers and principal components.

Conditional analysis of the GWAS with QC2 quality control for the QTPhenProxy EN model for all stroke identified 7 candidate variants with genome-wide significance, all which are novel, though some of the nearest genes to these loci have been identified in previous studies through nearby loci. There were 3 loci identified for the stroke subtype ischemic stroke, 3 loci for subarachnoid hemorrhage, and 3 loci for intracerebral hemorrhage (Table 3). Almost all of the genome-wide significant variants overlapped with those found running the GWAS using QC1 quality control. New variants that were genome-wide significant for all stroke included a deletion variant that was intergenic to the gene *ATP5MC1P3*, an intronic variant of the *MRSA* gene, and a 3'UTR variant in *KCNJ4* National Center for Biotechnology Information, National Library of Medicine.. In

bioRxiv preprint doi: https://doi.org/10.1101/2020.01.22.915397; this version posted January 23, 2020. The copyright holder for this preprint (which was not certified by peer review) is the author/funder, who has granted bioRxiv a license to display the preprint in perpetuity. It is made available under aCC-BY 4.0 International license.

addition, several genome-wide significant variants in the MEGASTROKE stroke and ischemic stroke GWAS were near the variants that were genome-wide significant in the QTPhenProxy EN GWAS. Almost all of those nearby MEGASTROKE genome-wide significant variants replicated to at least nominal significance of 0.05 in the QTPhenProxy EN GWAS (Table 4).

2.6. Effect sizes of QTPhenProxy and traditional binary trait analysis are correlated.

We determined the correlation between the effect sizes of the binary trait GWAS and QTPhenProxy GWAS. Pearson correlation of the beta coefficients and log of the odds ratios increased when restricting to variants with small p-values (max r^2=0.58 for GWAS with QC2 control, max r^2=0.70 for GWAS with QC1 control) (Figure 4, Supplementary Figure A.6). Too few variants, such as with p-values $>$ 5e-08 resulted in a decreased Pearson correlation.

2.7. Genome-wide significant variants are enirched in related EBI-GWAS marker sets.

From the over 2,000 EBI-GWAS disease variant marker sets mapped to organ systems, we calculated the proportion of markers in each set that was found to be at genome-wide significance by our QTPhenProxy model with QC2 markers and principal components. We found that the organ systems with markers sets with the highest proportion of genome-wide significant variants for stroke included vascular disorders, investigations, psychiatric disorders, and general disorders and administration site conditions (Figure A.5, Supplementary Figure 3). The enriched disease marker sets in the Investigations class included the lab values lipoprotein A levels, lipoprotein a levels adjusted for apolipoprotein A isoforms, blood protein levels, and white blood cell counts. The enriched disease marker sets

bioRxiv preprint doi: https://doi.org/10.1101/2020.01.22.915397; this version posted January 23, 2020. The copyright holder for this preprint (which was not certified by peer review) is the author/funder, who has granted bioRxiv a license to display the preprint in perpetuity. It is made available under aCC-BY 4.0 International license.

in the General disorders and administration site conditions included aortic valve stenosis and allergy, while the Psychiatric disorders enriched marker sets were response to statins (LDL change) and venous thromboembolism. For ischemic stroke, the top enriched disease marker sets included those described for stroke and also activated partial thromboplastin time, coagulation factor levels, protein biomarkers, soluble levels of adhesion molecules, pancreatic cancer, and urinary metabolites.

2.8. LD score regression intercept and genomic inflation are similar across stroke and its subtypes.

Using QC1 quality control, the genomic inflation for QTPhenProxy EN model for Stroke was 1.133, while using the QC2 quality control the genomic inflation for the same model was 1.134. For binary traits using QC2 quality control, genomic inflation for stroke was 1.027. Using the QC2 quality control model, the QTPhen-Proxy EN model genomic inflation for Ischemic stroke was 1.118, for subarachnoid hemorrhage was 1.122, and for intracerebral hemorrhage was 1.114. LD score regression intercept for QTPhenProxy EN model with QC2 quality control for stroke was 1.037 ± 0.0088, for ischemic stroke, 1.031 ± 0.0077, for subarachnoid hemorrhage, 1.012 ± 0.008, and for intracerebral hemorrhage, 1.051 ± 0.0081. We found that more common variants, or those with higher minor allele frequencies, had higher genomic inflation than rarer variants (Figure 4).

2.9. Simulation of conversion of quantitative trait to binary trait shows correlation of effect sizes to empirical data.

Based on the scale difference between binary and quantitative traits, the odds ratios are not directly comparable. We simulated the effect of a quantitative trait

bioRxiv preprint doi: https://doi.org/10.1101/2020.01.22.915397; this version posted January 23, 2020. The copyright holder for this preprint (which was not certified by peer review) is the author/funder, who has granted bioRxiv a license to display the preprint in perpetuity. It is made available under aCC-BY 4.0 International license.

locus and nearby marker both on the original quantitative trait and the binary trait converted from the quantitative trait using liability thresholding. We found high correlation of effect sizes between the beta coefficients and log odds ratios of the quantitative trait variants with p-value < 0.005 and their respective binary trait variant effect sizes (Pearson correlation, r^2=0.82). Lower p-values were not tested because of too few qualifying variants. After standard normalizing the quantitative trait, we also found the slope of the correlation between it and the log binary trait to be stable across the parameters, with a mean of 1.63 for each parameter except for marker allele frequency (1.35) and prevalence (1.77) (Supplementary Figure A.7).

3. Discussion

3.1. QTPhenProxy can identify patients with stroke using EHR data other than the disease diagnosis code.

For all stroke and its subtype ischemic stroke, the machine learning models trained to assign QTPhenProxy probabilities performed well (greater than 90% AUROC, greater than 30% maximum F1 score, 74-97% precision at 50). The models trained on subarachnoid hemorrhage and intracerebral hemorrhage cases performed similarly with AUROC but not as well with maximum F1 score and precision at 50. This may be due to the number of cases the two subtypes have to train on, which was an order of magnitude smaller (600 cases versus 3300-4300 cases). Importantly, we only trained on half of the cases and tested on the other half, which equates to 300-2200 cases, depending on the disease definition. From this small training set, we were able to assign a probability of disease to all 500,000 subjects in the UK Biobank. This training set is a fraction of the over 40,000 cases

bioRxiv preprint doi: https://doi.org/10.1101/2020.01.22.915397; this version posted January 23, 2020. The copyright holder for this preprint (which was not certified by peer review) is the author/funder, who has granted bioRxiv a license to display the preprint in perpetuity. It is made available under aCC-BY 4.0 International license.

required to power the most recent genome-wide association study for stroke (MEGASTROKE).

3.2. QTPhenProxy discovers many new variants and recovers known disease variants to genome-wide significance

Using QTPhenProxy resulted in 3-13 loci with genome-wide significance. In contrast, traditional binary trait GWAS using all disease cases resulted in the discovery of 0 genome-wide significant loci for stroke, ischemic stroke, and subarachnoid hemorrhage and 3 loci for intracerebral hemorrhage. In addition to new loci discovery, QTPhenProxy recovered known disease variants to a significance level of 0.05 with a sensitivity better than binary trait GWAS. In addition to recovering known variants, overall the effect size of the known variants in the binary trait GWAS was correlated with QTPhenProxy effect sizes for variants with low p-values. These results suggest that the QTPhenProxy method can recover relevant variants with fewer cases than traditional methods for stroke.

3.3. Simulation of quantitative trait and corresponding binary trait further supported the correlation of effect sizes between the two methods.

Our simulations showed high correlation between quantitative trait beta coefficients and binary trait log odds ratio, which is similar to our empirical findings in the UK Biobank. We also show that the correlation slope is relatively stable across all the different simulation parameters, suggesting that there is a set correlation between quantitative traits and binary traits created from them. Further simulation will need to determine the effects of multiple loci on correlation between quantitative and corresponding binary trait.

bioRxiv preprint doi: https://doi.org/10.1101/2020.01.22.915397; this version posted January 23, 2020. The copyright holder for this preprint (which was not certified by peer review) is the author/funder, who has granted bioRxiv a license to display the preprint in perpetuity. It is made available under aCC-BY 4.0 International license.

3.4. Variants discovered for stroke are enriched in disease marker sets for vascular and neurological disease, and variants discovered for other diseases were enriched for disease and system specific markers.

As a specificity measure for the variants discovered by QTPhenProxy, we found the EN model had the highest proportion of overlapping variants with EBI-GWAS marker sets related to vascular disorders and associated lab values. QT-PhenProxy variants improves the power of detecting variants related to diseases that are co-morbid or risk factors for stroke.

3.5. Low LD score regression intercepts relative to genomic inflation suggests high polygenicity.

Our genome-wide association studies using QTPhenProxy had moderate genomic inflation, slightly above 1.1, but low LD score regression intercepts near 1.0. The corresponding binary trait GWAS had genomic inflation below 1.05, suggesting minimal population stratification. Since the population for the binary trait GWAS was the same as those used for QTPhenProxy, this suggests that polygenicity, rather than population stratification, is the cause for genomic inflation. Polygenicity, or the contribution of small effects of many genes to a phenotype, may be the more likely cause Bulik-Sullivan et al. (2015). In addition, Bulik-sullivan et. al. argue that genomic inflation can increase with sample size when there is polygenicity, and LD score regression intercept is more robust in distinguishing inflated p-values from polygenicity. As seen in Howrigan et al. (2017), increased genomic inflation with common variants over rare variants suggests polygenicity. We show a similar upward trend in Figure 4. Another sign of true signal over inflated signal is the evidence of causal variants in linkage disequilibrium, as seen in a manhattan or hudson plot Howrigan et al. (2017).

bioRxiv preprint doi: https://doi.org/10.1101/2020.01.22.915397; this version posted January 23, 2020. The copyright holder for this preprint (which was not certified by peer review) is the author/funder, who has granted bioRxiv a license to display the preprint in perpetuity. It is made available under aCC-BY 4.0 International license.

Figure 2 shows genome-wide significant variants in linkage disequilibrium with each other. Finally, this study reports results from using two different quality controls in the genome-wide association analysis, QC1, and more stringent, QC2. Results using QC1 showed more variants with genome-wide significance and discovered more new variants for stroke than the QC2 GWAS. This may lead one to believe that more stringent quality control led to reduced inflation of p-values. However, the genomic inflation of the p-values from the QC1 GWAS was the same as the genomic inflation of the p-values from the QC2 GWAS (1.134 vs 1.133) with the QC2 GWAS having a slightly higher LD score regression intercept value (1.0288 vs 1.0369). This suggests that the p-values from the QC1 GWAS may not by overly inflated.

3.6. QTPhenProxy replicates known stroke variants and discovers variants within cardiovascular disease genes.

Several of the genes discovered by the QTPhenProxy GWAS, using QC1 or QC2 quality control have been associated with stroke, including *NOS3*, *FURIN*, *PITX2*, *CDK2NB*, *LDLR*, and *ABO* Malik et al. (2018a,b). *NOS3*, in particular was discovered through meta-analysis of the MEGASTROKE results with the UK Biobank Malik et al. (2018b). We were able to replicate this association using only the QTPhenProxy method on the UK Biobank, and not traditional binary trait analysis. *NOS3* has been shown to be related to hypertension either through salt excretion regulation in the kidney Gao Yang et al. (2018) or regulation of vascular relaxation in endothelial cells Farah et al. (2018). Other discovered genes by QTPhenProxy are also associated with related cardiovascular diseases. *F5* gene codes for an essential coagulation factor, and mutations that can lead to increased thrombosis or hemorrhage, depending on the mutation Asselta and Peyvandi

bioRxiv preprint doi: https://doi.org/10.1101/2020.01.22.915397; this version posted January 23, 2020. The copyright holder for this preprint (which was not certified by peer review) is the author/funder, who has granted bioRxiv a license to display the preprint in perpetuity. It is made available under aCC-BY 4.0 International license.

(2009); Kujovich (2011); Hinds et al. (2016). *LPA* codes for a protein, lipoprotein-A, that can contribute to atherosclerosis Song et al. (2019); Wang Long et al. (2016). Mutations in the *PLCB1* gene, which encodes for phospholipase synthesis, have been found in epilepsy and seizures Schoonjans et al. (2016). *LDLR* gene codes for the low-density lipoprotein receptor, which is involved in cholesterol production Biobank, and the *APOC1*/*APOC1P1* genes code for parts of apoliprotein C1, which are involved in high density lipoprotein metabolism Erqou et al. (2010). *ARHGAP1*, a gene coding for Rho GTPase activating protein 1 has been associated with cancer phenotypes and activation of hypoxic and inflammatory pathways Fessler et al. (2004); Hashimoto et al. (2018); Zhang et al. (2019). *ABCG8* gene has been associated with combined gwas of lipids and inflammation, lipid levels, and gallstone disease Ligthart et al. (2016). *EYST3* and *XKR6* gene mutations have been associated with coronary artery disease and ischemic stroke respectively in Asian populations, and *MRAS* gene mutations have been associated with coronary artery disease in two populations Jiang et al. (2011); Zheng et al. (2019); Song et al. (2019); Erdmann et al. (2009). These results suggest that QTPhenProxy has replicated genome-wide significant mutations in genes known to be related with stroke and discovered of those associated with related risk factors such as coronary artery neurological diseases. Out of the 13 newly discovered variants with genome-wide significance, five are intronic or nearby genes that have been found in previous studies (MEGASTROKE), and five more are have been discovered in previous GWAS studies of related cardiovascular diseases. The variants within and near the *F5* gene had the highest genetic signal for stroke and all of its subtypes, even though it was not replicated in the MEGASTROKE GWAS. Out of all the new variants discovered by the QTPhenProxy EN model using the GWAS QC2

bioRxiv preprint doi: https://doi.org/10.1101/2020.01.22.915397; this version posted January 23, 2020. The copyright holder for this preprint (which was not certified by peer review) is the author/funder, who has granted bioRxiv a license to display the preprint in perpetuity. It is made available under aCC-BY 4.0 International license.

quality control, the rs11887534 variant, a missense mutation within the *ABCG8* gene, replicated to a p-value significance of 6.85E-04 in the MEGASTROKE stroke GWAS of over 40,000 European ancestry subjects. Using a tenth of the number of cases, QTPhenProxy discovered a variant within a new gene that replicated in MEGASTROKE, and discovered variants within known stroke genes.

3.7. Limitations

There are several limitations with this method. First, out of the five machine learning models used in QTPhenProxy, only two provided probabilities along a continuous scale. Adaboost, gradient boosting, and logistic regression using L1 penalty models, although with high performance, assigned probabilities in discrete bins. These distributions violate the the genome-wide association linear regression assumption of normal distribution of the quantitative trait. Although the probabilities produced by EN and RF models were not initially normally distributed, they were continuous, and could be adjusted with quantile normalization. In addition, the GWAS results from QTPhenProxy using the RF model resulted in many more hits than the EN model, and reduced sensitivity to known disease variants. Further study will be required to understand why one model gave more sensitive and specific results than the other, and whether there was p-value inflation in the random forest models. QTPhenProxy also may be particularly suited for stroke because the training model for phenotyping patients was optimized for stroke Thangaraj et al. (2019). Since stroke is an acute event than can be identified with high accuracy in the electronic health record, this method may not translate as well to other diseases, such as chronic illnesses. Another potential limitation of the study is that only about half of known loci for stroke are replicated with significance of less than 0.05 in the QTPhenProxy method, even though new

bioRxiv preprint doi: https://doi.org/10.1101/2020.01.22.915397; this version posted January 23, 2020. The copyright holder for this preprint (which was not certified by peer review) is the author/funder, who has granted bioRxiv a license to display the preprint in perpetuity. It is made available under aCC-BY 4.0 International license.

variants are suggested.

3.8. Conclusions

We have developed a method, QTPhenProxy, that we have shown improves the power of genome-wide association studies in stroke and three of its subtypes: ischemic stroke, subarachnoid hemorrhage, and intracerebral hemorrhage with an order of magnitude fewer cases than required for traditional genome-wide association studies of the same diseases. Converting dichotomous traits to quantitative ones could result in improvement of power by incorporating electronic health record information for subjects who may have genetic susceptibility to stroke but may not have experience a stroke yet. Previous studies have shown that for diseases with low prevalence, there can be a reduction of power using logistic regression for binary trait GWAS compared to linear regression for quantitative trait GWAS Zaitlen et al. (2012). Recently, Abraham et al. (2019) showed that the inclusion of ischemic stroke risk factors' genome-wide significant SNPs in polygenic risk score improves prediction of ischemic stroke. This supports our idea that inclusion of risk factor information into the phenotype can hep detect genetically susceptible subjects. We show that with as few as 2200 stroke subjects we can recover known variants of stroke and discover new variants that have been linked to cardiovascular and nervous system diseases. This method could be useful for studies with a small set of cases and without access to large meta-analyses. We also have suggested new variants that warrant further replication in other groups. QTPhenProxy shows the benefits of incorporating electronic health record data to convert traditional binary traits to quantitative in improving GWAS power.

bioRxiv preprint doi: https://doi.org/10.1101/2020.01.22.915397; this version posted January 23, 2020. The copyright holder for this preprint (which was not certified by peer review) is the author/funder, who has granted bioRxiv a license to display the preprint in perpetuity. It is made available under aCC-BY 4.0 International license.

4. Acknowledgements

All UK Biobank data analysis conducted in this work is available upon request. I would like to thank Dr. Krzysztof Kiryluk, Dr. Konrad Karczewski, Jie Yuan, Dr. Anna O. Basile for helpful discussions and guidance. Thank you also to Dr. Anna O. Basile, Nicholas Giangreco, and Jenna Kefeli for assistance in the UK Biobank application. This research has been conducted using the UK Biobank Resource under Application Number 41039. PT is funded by F30HL140946, and NT is funded by R35GM131905 and was funded by 5R01GM107145. MedDRA® trademark is registered by IFPMA on behalf of ICH. The MEGASTROKE project received funding from sources specified at http://www.megastroke.org/acknowledgments.html.

5. Author Contributions

Conceptualization: P.T. and N.T., methodology: P.T and N.T., software: P.T. and N.T., formal analysis: P.T. and N.T., investigation: P.T. and N.T., resources: P.T. and N.T., data curation: P.T. and N.T., writing-original draft: P.T. and N.T., writing-review and editing: P.T. and N.T., visualization: P.T and N.T, Supervision: N.T., Funding Acquisition: P.T. and N.T.

6. Declaration of Interests

The authors declare no competing interests.

bioRxiv preprint doi: https://doi.org/10.1101/2020.01.22.915397; this version posted January 23, 2020. The copyright holder for this preprint (which was not certified by peer review) is the author/funder, who has granted bioRxiv a license to display the preprint in perpetuity. It is made available under aCC-BY 4.0 International license.

7. Figures

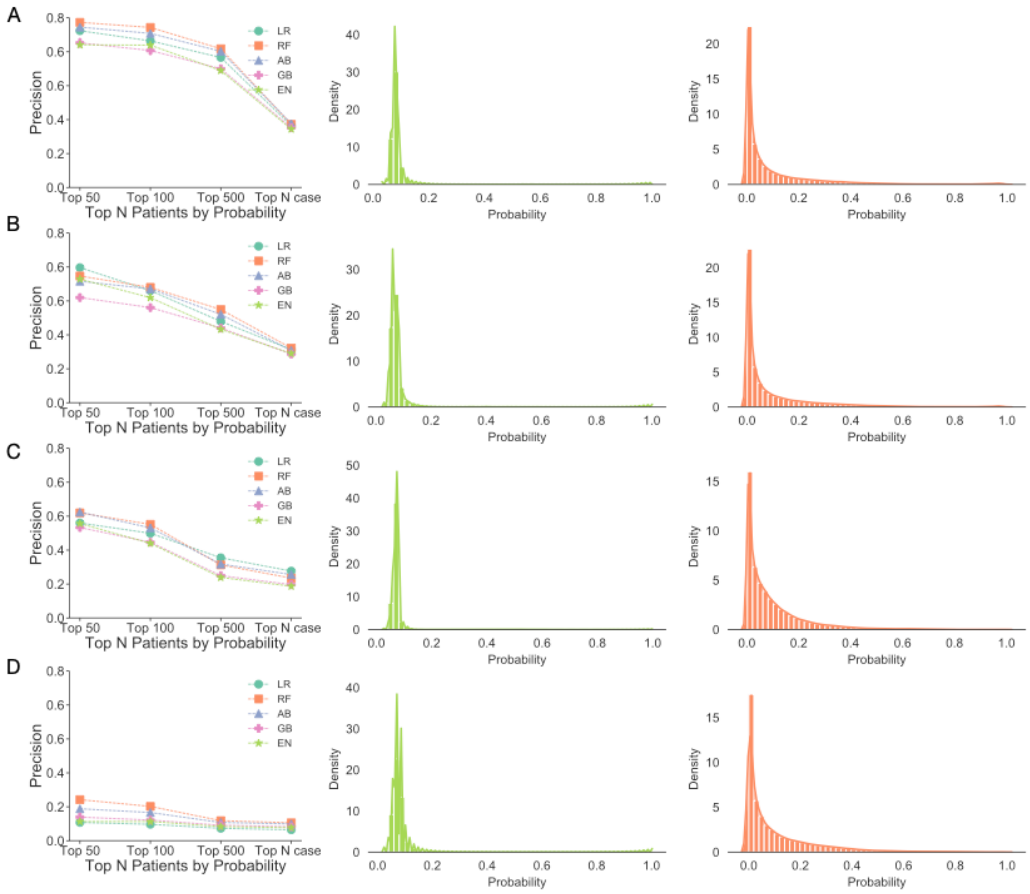

Figure 1: **Precision at top 50, 100, 500, and N cases probabilities assigned by machine learning algorithms on hold out test set and probability distributions.** A. All Stroke, B. Ischemic Stroke, C. Sub-arachnoid Hemorrhage, D. Intracerebral Hemorrhage. Left panel: Precision of each algorithm Circles represent precision for the Logistic Regression model with L1 penalty (LR), squares: Random Forest model (RF), triangles: Adaboost model (AB), cross: Gradient boosting model (GB), and star Logistic Regression model with Elastic Net penalty (EN). Middle Panel: EN probability distributions, Right panel: RF Probability distributions

bioRxiv preprint doi: https://doi.org/10.1101/2020.01.22.915397; this version posted January 23, 2020. The copyright holder for this preprint (which was not certified by peer review) is the author/funder, who has granted bioRxiv a license to display the preprint in perpetuity. It is made available under aCC-BY 4.0 International license.

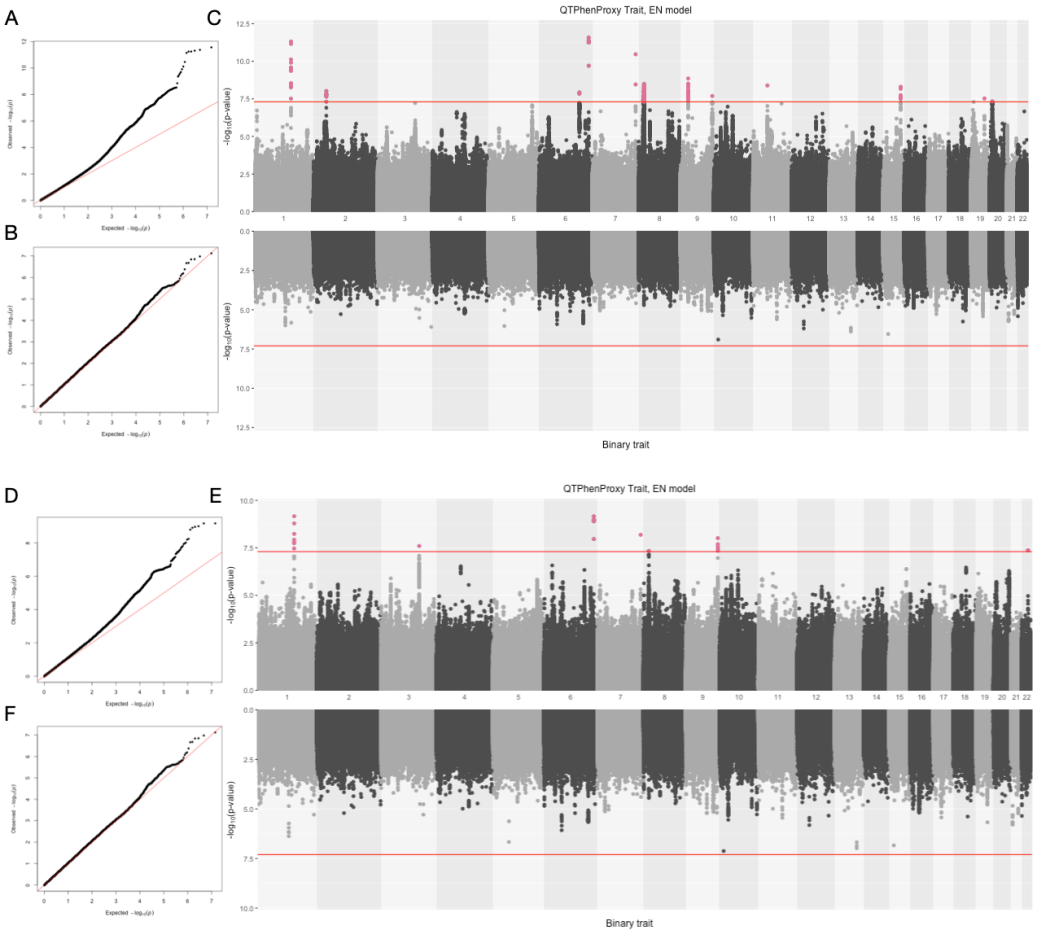

Figure 2: **QQ Plots and Hudson plot of QTPhenProxy genome-wide association analysis, EN Model with Binary trait genome-wide association analysis for Stroke, (Top) using QC1 quality control and (Bottom) using QC2 quality control.** A. and D. Q-Q Plot for QTPhenProxy, EN Model GWAS. B.and E. Q-Q Plot for Binary trait GWAS. C. and F. Top manhattan plot is for QTPhenProxy, bottom plot for binary trait.Variants with p-value $<$ 5e-08 are highlighted in pink, and the dashed lines are at the same value.

bioRxiv preprint doi: https://doi.org/10.1101/2020.01.22.915397; this version posted January 23, 2020. The copyright holder for this preprint (which was not certified by peer review) is the author/funder, who has granted bioRxiv a license to display the preprint in perpetuity. It is made available under aCC-BY 4.0 International license.

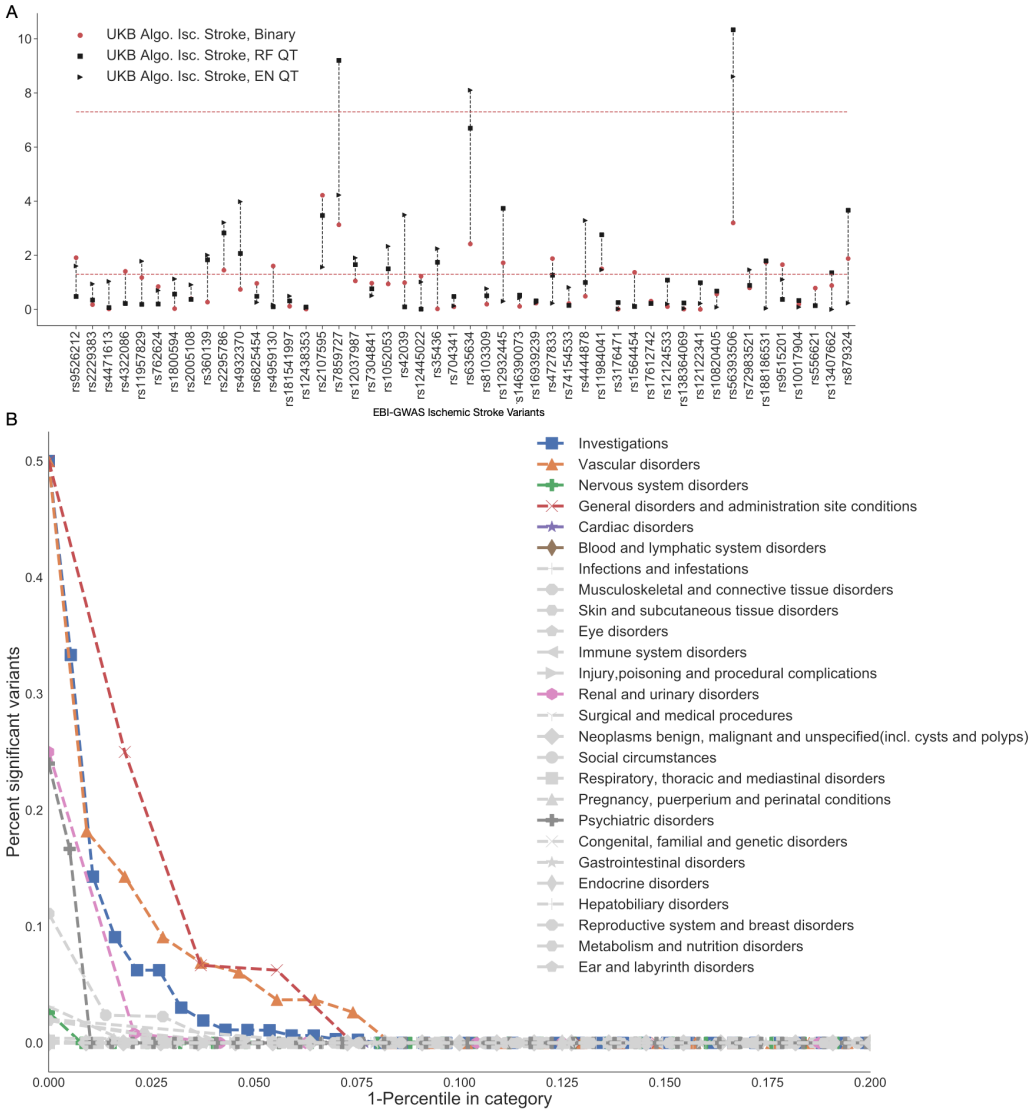

Figure 3: **QTPhenProxy recovers known ischemic stroke variants and variants specific to related organ systems.** Results from QTPhenProxy GWAS with QC2 quality control. (A) Horizontal axis shows Ischemic Stroke variants catalogued in EBI-GWAS that have shown genome-wide significance in previous studies. Black markers represent p-values of variants recovered by QTPhenProxy models (square=RF,Triangle=EN). (B) X-axis is the top percentile of marker sets in each category, Y-axis is the proportion of variants in marker sets that overlap with QTPhenProxy genome-wide significant variants. Each shape corresponds to a disease category. In color are top disease categories: Square=Investigations, Triangle=Vascular disorders, Cross=Nervous system disorders, X=General disorders and administration site conditions, Star=cardiac disorders, and Diamond=Blood and lymphatic system disorders.

bioRxiv preprint doi: https://doi.org/10.1101/2020.01.22.915397; this version posted January 23, 2020. The copyright holder for this preprint (which was not certified by peer review) is the author/funder, who has granted bioRxiv a license to display the preprint in perpetuity. It is made available under aCC-BY 4.0 International license.

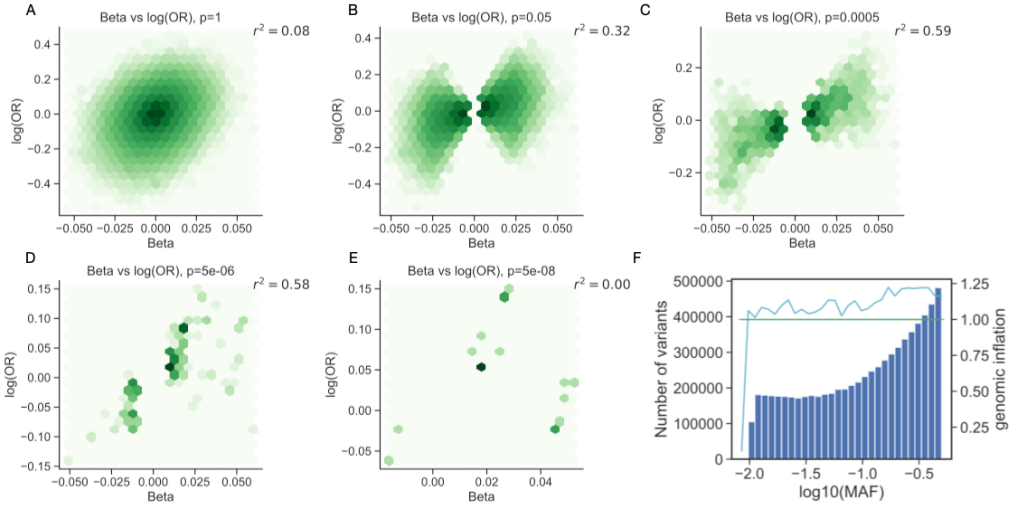

Figure 4: **Correlation between beta and odds ratio effect sizes for variants at varying degrees of significance and Genomic Inflation within bins of variants with similar minor allele frequencies for QTPhenProxy EN Model for Stroke with QC2 quality control.** (A-E) Correlation between QTPhenProxy, EN Model for Stroke GWAS and Binary trait GWAS effect size, QC2 quality control. X-axis is QTPhenProxy GWAS beta-coefficients, Y-axis is log base 10 of the Binary GWAS odds ratios. Pearson correlation is recorded in top right corner. From left to right, top to bottom, variants included decreases by restricting p-value.(F) Genomic Inflation within bins of variants with similar minor allele frequencies for QTPhenProxy EN Model for Stroke with QC2 quality control. Light blue line shows the genomic inflation of each bin of variants, green line shows 1.0 genomic inflation, and blue bars show numbers of SNPs (variants) in each bin, binned by *log10(MAF)*, or log(minor allele frequency.)

bioRxiv preprint doi: https://doi.org/10.1101/2020.01.22.915397; this version posted January 23, 2020. The copyright holder for this preprint (which was not certified by peer review) is the author/funder, who has granted bioRxiv a license to display the preprint in perpetuity. It is made available under aCC-BY 4.0 International license.

8. Tables

Disease	N Cases	Binary Hits	Bin Sens	RF Hits	RF Sens	EN Hits	EN Sens
Stroke	4354	0	0.217	1215	0.217	120	0.261
IscStroke	3308	0	0.312	1266	0.312	202	0.333
SAHStroke	665	0	NA	722	NA	69	NA
ICHStroke	581	2	NA	1059	NA	146	NA

Table 1: **Number of genome-wide significant loci and proportion of known stroke variants that reach nominal significance for each model.** *IscStroke*: Ischemic Stroke, *SAHStroke*: Subarachnoid Hemorrhage, *ICHStroke*: Intracerebral Hemorrhage, *N Cases*: number of cases, *hits*: Number of genome-wide significant loci, *sens*: sensitivity measure for each model GWAS and binary trait GWAS, measures what proportion of known stroke variants reach genome-wide significance in each association test. *RF*: Random Forest model, *EN*: Logistic Regression with elastic net penalty model.

Phenotype	rsID	Chr.	Gene	Location	R/R allele	RAF	Beta	Converted OR	P value
Stroke	rs6025	1q24.2	*F5*	missense	T/C	0.0231	0.0492 (0.0421-0.0564)	1.09 (1.08-1.10)	**4.87e-12**
Stroke	rs8179838	2p21	*MTA3*	intronic	T/C	0.621	0.0126 (0.0104-0.0149)	1.02 (1.02-1.03)	**9.63e-09**
Stroke	rs6923947	6q22.32	*LOC105377992*	intergenic	A/G	0.447	0.0123 (0.0101-0.0144)	1.02 (1.02-1.02)	**1.19e-08**
Stroke	rs55730499	6q25.3	*LPA*	intronic	T/C	0.0817	0.0273 (0.0234-0.0312)	1.05 (1.04-1.06)	**2.70e-12**
Stroke	rs3918226	7q36.1	*NOS3*	intronic	T/C	0.0814	0.0263 (0.0223-0.0302)	1.05 (1.04-1.05)	**3.44e-11**
Stroke	rs6991641	8p23.1	*SOX7*	intronic	G/C	0.403	0.013 (0.0108-0.0152)	1.02 (1.02-1.03)	**3.29e-09**
Stroke	rs1333049	9p21.3	*CDKN2A-CDKN2B*	intergenic	C/G	0.481	0.0129 (0.0108-0.0151)	1.02 (1.02-1.03)	**1.41e-09**
Stroke	9:136138765	9q34.3	*ABO*	intronic	G/GC...	0.184	0.0155 (0.0128-0.0183)	1.03 (1.02-1.03)	**2.05e-08**
Stroke	11:46705193	11p11.2	*ARHGAP1*	intronic	C/CT	0.28	0.0143 (0.0119-0.0167)	1.02 (1.02-1.03)	**4.10e-09**
Stroke	rs59065675	15q26.1	*FURIN*	intronic	C.../C	0.47	0.0127 (0.0105-0.0149)	1.02 (1.02-1.03)	**5.00e-09**
Stroke	rs814573	19q13.32	*APOC1-APOC1P1*	intergenic	T/A	0.188	0.0156 (0.0128-0.0184)	1.03 (1.02-1.03)	**2.97e-08**
Stroke	20:862958	20p12.3	*PLCB1*	intronic	TA/T	0.76	0.0138 (0.0113-0.0164)	1.02 (1.02-1.03)	**4.73e-08**

bioRxiv preprint doi: https://doi.org/10.1101/2020.01.22.915397; this version posted January 23, 2020. The copyright holder for this preprint (which was not certified by peer review) is the author/funder, who has granted bioRxiv a license to display the preprint in perpetuity. It is made available under aCC-BY 4.0 International license.

IscStroke	rs1894692	1q24.2	*F5-SLC19A2*	intergenic	G/A	0.0218	0.0546 (0.0478-0.0614)	1.1 (1.09-1.11)	**8.22e-16**
IscStroke	rs369787256	4q25	*PITX2-MIR297*	intergenic	C/T	0.0905	0.0223 (0.0188-0.0257)	1.04 (1.03-1.05)	**1.17e-10**
IscStroke	rs55730499	6q25.3	*LPA*	intronic	T/C	0.0817	0.0272 (0.0236-0.0307)	1.05 (1.04-1.05)	**2.49e-14**
IscStroke	rs117733303	6q25.3	*LPAL2*	intronic	G/A	0.0187	0.0428 (0.0356-0.05)	1.08 (1.06-1.09)	**2.69e-09**
IscStroke	rs3918226	7q36.1	*NOS3*	intronic	T/C	0.0814	0.0209 (0.0173-0.0246)	1.04 (1.03-1.04)	**6.81e-09**
IscStroke	rs2205258	8q23.3	*LOC107986968*	intronic	C/T	0.83	0.0151 (0.0125-0.0177)	1.03 (1.02-1.03)	**6.76e-09**
IscStroke	rs8176719	9q34.2	*ABO*	insertion	TC/T	0.34	0.0145 (0.0124-0.0165)	1.02 (1.02-1.03)	**2.17e-12**
IscStroke	rs1333049	9p21.3	*CDKN2A-CDKN2B*	intergenic	C/G	0.481	0.0132 (0.0112-0.0151)	1.02 (1.02-1.03)	**1.31e-11**
IscStroke	11:46705193	11p11.2	*ARHGAP1*	intronic	C/CT	0.28	0.0122 (0.01-0.0145)	1.02 (1.02-1.02)	**3.22e-08**
IscStroke	rs814573	19q13.32	*APOC1-APOC1P1*	intergenic	T/A	0.188	0.0172 (0.0146-0.0198)	1.03 (1.02-1.03)	**1.85e-11**
IscStroke	rs118068660	19p13.2	*LDLR*	intergenic	C/T	0.901	0.0193 (0.0159-0.0227)	1.03 (1.03-1.04)	**1.43e-08**
IscStroke	rs12151925	20p12.2	*LOC101929413-FAT1P1*	intergenic	C/T	0.222	0.0129 (0.0105-0.0152)	1.02 (1.02-1.03)	**4.26e-08**
SAHStroke	rs6025	1q24.2	*F5*	missense	T/C	0.0231	0.0673 (0.0593-0.0753)	1.12 (1.11-1.14)	**4.61e-17**
SAHStroke	rs36058710	9q34.2	*ABO*	intronic	CT/C	0.287	0.0166 (0.0139-0.0194)	1.03 (1.02-1.03)	**1.03e-09**
SAHStroke	rs34850248	12q12	*LINC02400*	intergenic	A/AC	0.0714	0.0268 (0.0221-0.0314)	1.05 (1.04-1.06)	**9.95e-09**
ICHStroke	rs6025	1q24.2	*F5*	missense	T/C	0.0231	0.0480 (0.0411-0.0549)	1.09 (1.07-1.1)	**2.85e-12**
ICHStroke	rs11887534	2p21	*ABCG8*	missense	G/C	0.935	0.0271 (0.0229-0.0313)	1.05 (1.04-1.06)	**7.90e-11**
ICHStroke	rs372302634	3q22.3	*ESYT3-MRAS*	intergenic	T/T...	0.457	0.0121 (0.01-0.0142)	1.02 (1.02-1.02)	**8.51e-09**
ICHStroke	rs6923947	6q22.32	*LOC105377992*	intergenic	A/G	0.447	0.0127 (0.0106-0.0148)	1.02 (1.02-1.03)	**9.5e-10**
ICHStroke	rs2077111	6q22.33	*RPS4XP9*	intergenic	G/A	0.447	0.012 (0.00995-0.0141)	1.02 (1.02-1.02)	**8.89e-09**
ICHStroke	rs1808593	7q36.1	*NOS3*	intronic	G/T	0.25	0.0131 (0.0107-0.0155)	1.02 (1.02-1.03)	**4.14e-08**
ICHStroke	rs7013277	8p23.1	*XKR6*	intronic	C/A	0.396	0.0116 (0.00947-0.0137)	1.02 (1.02-1.02)	**4.6e-08**
ICHStroke	11:46705193	11p11.2	*ARHGAP1*	intronic	C/CT	0.28	0.0133 (0.011-0.0156)	1.02 (1.02-1.03)	**1.35e-08**

Table 2: **Genome-wide significant variants discovered by QTPhenProxy, EN Model, using QC1 quality control.** Cytogenic position was determined using Kent et al. (2002). *rsID*: variant id, *Chr*: cytogenic position, *Location*: location of variant relative to the gene, *R/R*: risk/reference, *RAF*: risk allele frequency in population, *Beta*: Beta coefficient *OR*: Odds Ratio, 95% Confidence Intervals

Phenotype	rsID	Chr.	Gene	P value	MEGASTROKE P value
Stroke	rs1894692	1q24.2	*F5-SLC19A2*	**6.87E-10**	0.435

bioRxiv preprint doi: https://doi.org/10.1101/2020.01.22.915397; this version posted January 23, 2020. The copyright holder for this preprint (which was not certified by peer review) is the author/funder, who has granted bioRxiv a license to display the preprint in perpetuity. It is made available under aCC-BY 4.0 International license.

Stroke	rs8179838	2p21	*MTA3*	8.36E-06	0.515
Stroke	rs769407520	3q22.3	*ATP5MC1P3*	**2.50E-08**	not found
Stroke	rs6923947	6q22.32	*LOC105377992*	4.58E-07	0.04332
Stroke	rs55730499	6q25.3	*LPA*	**6.85E-10**	0.05915
Stroke	rs3918226	7q36.1	*NOS3*	**6.45E-09**	0.00134
Stroke	8:10206921	8p23.1	*MSRA*	**4.62E-08**	not found
Stroke	rs1333049	9p21.3	*CDKN2A-CDKN2B*	5.02E-06	1.85E-07
Stroke	9:136138765	9q34.3	*ABO*	**9.73E-09**	not found
Stroke	11:46705193	11p11.2	*ARHGAP1*	7.06E-07	not found
Stroke	rs59065675	15q26.1	*FURIN*	4.06E-07	not found
Stroke	rs814573	19q13.32	*APOC1-APOC1P1*	2.52E-05	0.412
Stroke	20:862958	20p12.3	*PLCB1*	1.95E-06	not found
Stroke	rs2269608	22q13.1	*KCNJ4*	**4.23E-08**	0.212
IscStroke	rs1894692	1q24.2	*F5-SLC19A2*	**1.90E-11**	0.229
IscStroke	rs369787256	4q25	*PITX2-MIR297*	3.69E-06	not found
IscStroke	rs55730499	6q25.3	*LPA*	**1.26E-09**	0.0316
IscStroke	rs117733303	6q25.3	*LPAL2*	0.000119	0.422
IscStroke	rs3918226	7q36.1	*NOS3*	3.59E-06	0.00118
IscStroke	rs2205258	8q23.3	*LOC107986968*	7.16E-06	0.415
IscStroke	9:1361387	9q34.2	*ABO*	**4.99E-10**	not found
IscStroke	rs1333049	9p21.3	*CDKN2A-CDKN2B*	3.01E-06	1.09E-06
IscStroke	11:46705193	11p11.2	*ARHGAP1*	3.85E-05	not found
IscStroke	rs814573	19q13.32	*APOC1-APOC1P1*	2.20E-06	0.716
IscStroke	rs118068660	19p13.2	*LDLR*	1.28E-06	1.14E-05

bioRxiv preprint doi: https://doi.org/10.1101/2020.01.22.915397; this version posted January 23, 2020. The copyright holder for this preprint (which was not certified by peer review) is the author/funder, who has granted bioRxiv a license to display the preprint in perpetuity. It is made available under aCC-BY 4.0 International license.

IscStroke	rs12151925	20p12.2	*LOC101929413-FAT1P1*	0.000107	0.104
SAHStroke	rs6025	1q24.2	*F5*	**6.34E-18**	0.453
SAHStroke	rs36058710	9q34.2	*ABO*	**1.59E-10**	not found
SAHStroke	rs34850248	12q12	*LINC02400*	**7.18E-09**	not found
ICHStroke	rs6025	1q24.2	*F5*	**1.52E-10**	0.453
ICHStroke	rs11887534	2p21	*ABCG8*	**4.29E-08**	6.85E-04
ICHStroke	rs372302634	3q22.3	*ESYT3-MRAS*	**4.03E-08**	not found
ICHStroke	rs6923947	6q22.32	*LOC105377992*	1.47E-07	0.00433
ICHStroke	rs2077111	6q22.33	*RPS4XP9*	1.96E-06	0.0372
ICHStroke	rs1808593	7q36.1	*NOS3*	2.96E-06	0.565
ICHStroke	rs7013277	8p23.1	*XKR6*	2.06E-05	0.156
ICHStroke	11:46705193	11p11.2	*ARHGAP1*	3.59E-06	not found

Table 3: **Genome-wide significant variants discovered by QTPhenProxy, EN Model, using QC2 quality control.** Also includes QC2 p-value for genome-wide significant variants from QC1 GWAS and p-values for variants from the MEGASTROKE stroke or ischemic stroke european GWAS Malik et al. (2018a). Cytogenic position was determined using Kent et al. (2002). *rsID*: variant id, *Chr*: cytogenic position

bioRxiv preprint doi: https://doi.org/10.1101/2020.01.22.915397; this version posted January 23, 2020. The copyright holder for this preprint (which was not certified by peer review) is the author/funder, who has granted bioRxiv a license to display the preprint in perpetuity. It is made available under aCC-BY 4.0 International license.

Phenotype	Gene	rsID	QTPhenProxy p-value
Stroke	*LPA*	rs56393506	1.09E-08
Stroke	*NOS*	rs1799983	not found
Stroke	*CDKN2B-CDKN2A*	rs7859727	6.94E-05
Stroke	*ABO*	rs635634	1.07E-07
Stroke	*FURIN*	rs4932370	2.55E-05
Stroke	*COL4A1*	rs9521634	0.00375
Stroke	*LOC105372798*	rs720470	0.88
Ischemic stroke	*PITX2-MIR297*	rs13143308	not found
Ischemic stroke	*LPA*	rs56393506	2.50E-09
Ischemic stroke	*NOS3*	rs1799983	not found
Ischemic stroke	*CDKN2B-CDKN2A*	rs7859727	5.95E-05
Ischemic stroke	*ABO*	rs635634	7.93E-09
Ischemic stroke	*LDLR*	rs8103309	0.171
Subarachnoid Hemorrhage	*ABO*	rs635634	2.22E-06
Intracerebral Hemorrhage	*NOS3*	rs1799983	not found

Table 4: **QTPhenProxy EN Model GWAS using QC2 quality control P-value of variants that were genome-wide significant in MEGASTROKE Stroke and Ischemic Stroke GWAS.**

bioRxiv preprint doi: https://doi.org/10.1101/2020.01.22.915397; this version posted January 23, 2020. The copyright holder for this preprint (which was not certified by peer review) is the author/funder, who has granted bioRxiv a license to display the preprint in perpetuity. It is made available under aCC-BY 4.0 International license.

Appendix A. Supplementary Figures

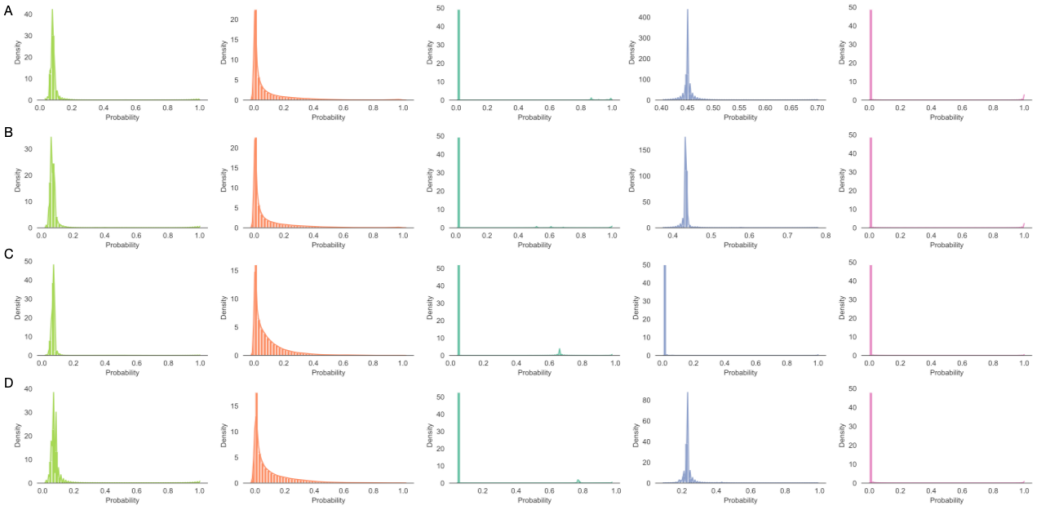

Figure A.1: **Model probability distributions assigned by machine learning algorithms, related to Figure 1.** A. All Stroke, B. Ischemic Stroke, C. Sub-arachnoid Hemorrhage, D. Intracerebral Hemorrhage. First panel: Logistic Regression model with Elastic Net penalty probabiltiy distribution, Second panel: Random Forest probability distribution, Third panel: Logistic Regression model with L1 penalty probability distribution, Fourth panel: Adaboost probability distribution, Fifth panel: Gradient boosting probability distribution

bioRxiv preprint doi: https://doi.org/10.1101/2020.01.22.915397; this version posted January 23, 2020. The copyright holder for this preprint (which was not certified by peer review) is the author/funder, who has granted bioRxiv a license to display the preprint in perpetuity. It is made available under aCC-BY 4.0 International license.

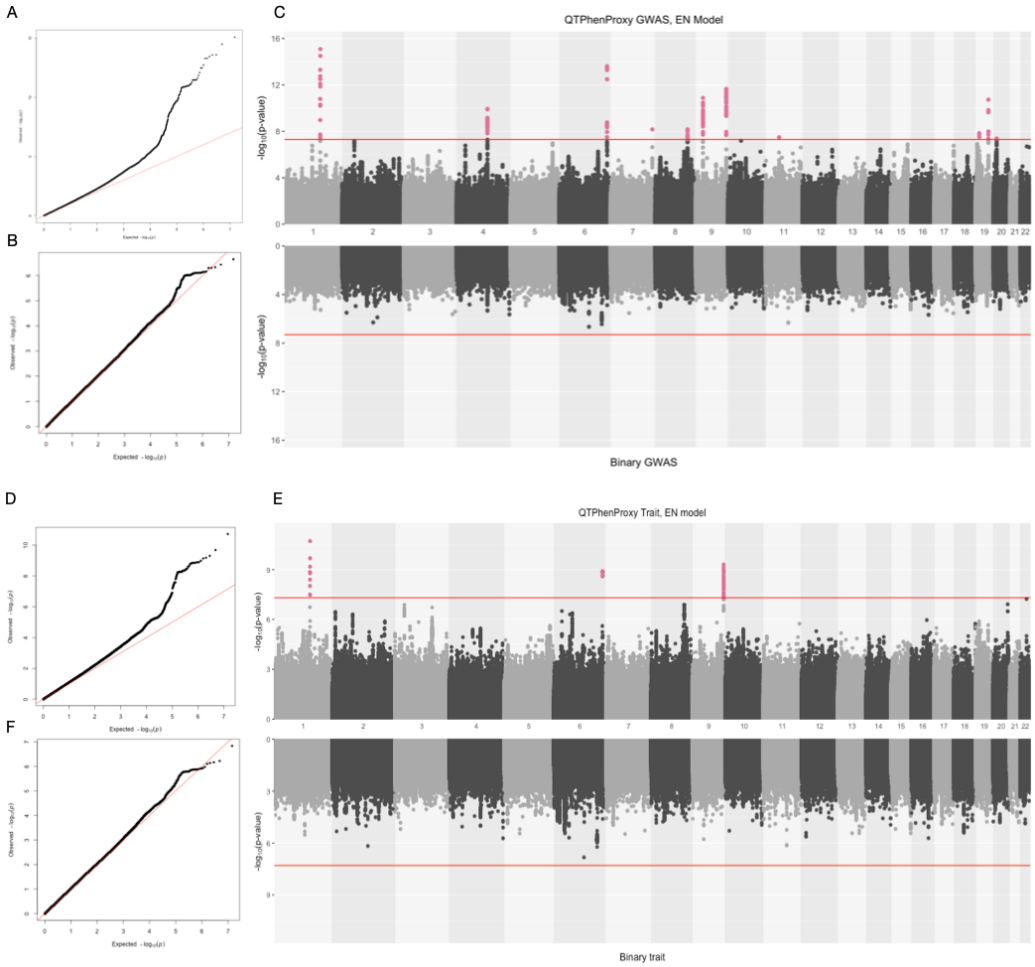

Figure A.2: **QQ Plots and Hudson plot of QTPhenProxy genome-wide association analysis, EN Model with Binary trait genome-wide association analysis for Ischemic Stroke, (Top) using QC1 quality control and (Bottom) using QC2 quality control, related to Figure 2.** A. and D. Q-Q Plot for QTPhenProxy, EN Model GWAS. B.and E. Q-Q Plot for Binary trait GWAS. C. and F. Top manhattan plot is for QTPhenProxy, bottom plot for binary trait.Variants with p-value $<$ 5e-08 are highlighted in pink, and the dashed lines are at the same value.

bioRxiv preprint doi: https://doi.org/10.1101/2020.01.22.915397; this version posted January 23, 2020. The copyright holder for this preprint (which was not certified by peer review) is the author/funder, who has granted bioRxiv a license to display the preprint in perpetuity. It is made available under aCC-BY 4.0 International license.

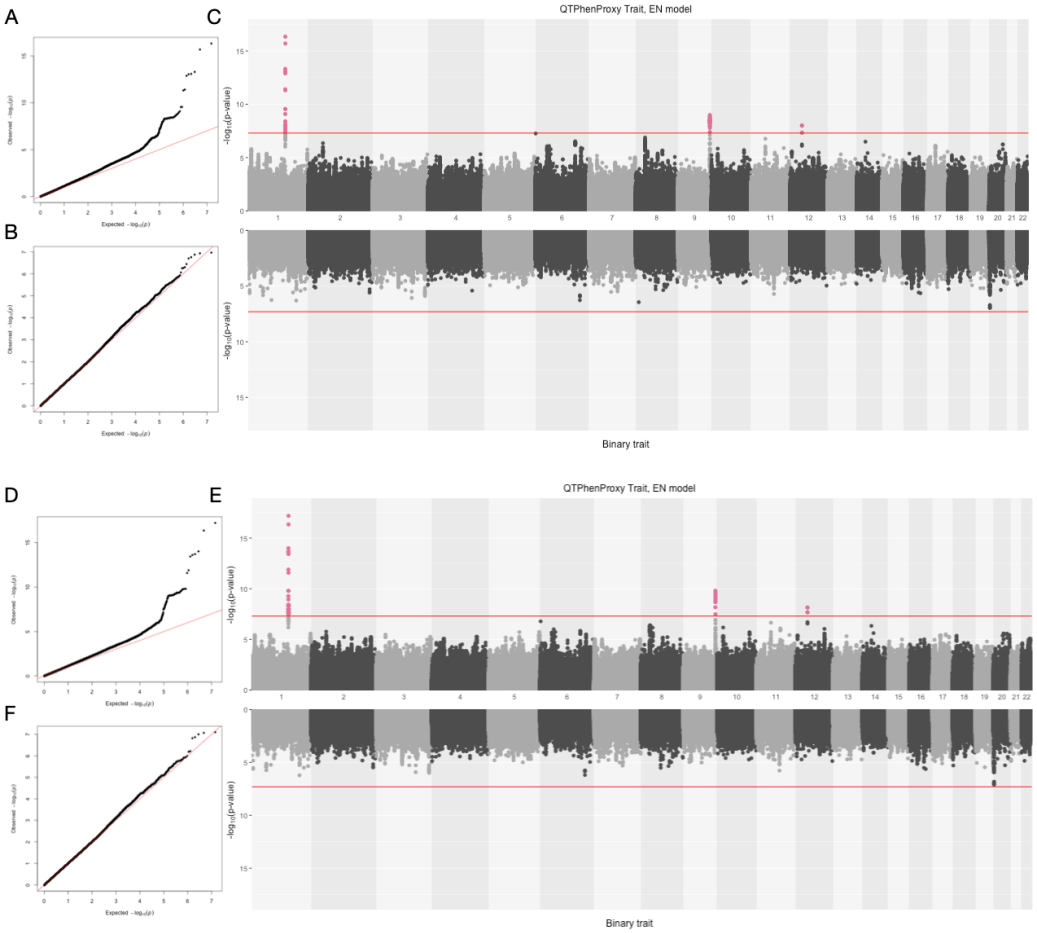

Figure A.3: **QQ Plots and Hudson plot of QTPhenProxy genome-wide association analysis, EN Model with Binary trait genome-wide association analysis for Subarachnoid Hemorrhage, (Top) using QC1 quality control and (Bottom) using QC2 quality control, related to Figure 2.** A. and D. Q-Q Plot for QTPhenProxy, EN Model GWAS. B.and E. Q-Q Plot for Binary trait GWAS. C. and F. Top manhattan plot is for QTPhenProxy, bottom plot for binary trait.Variants with p-value $<$ 5e-08 are highlighted in pink, and the dashed lines are at the same value.

bioRxiv preprint doi: https://doi.org/10.1101/2020.01.22.915397; this version posted January 23, 2020. The copyright holder for this preprint (which was not certified by peer review) is the author/funder, who has granted bioRxiv a license to display the preprint in perpetuity. It is made available under aCC-BY 4.0 International license.

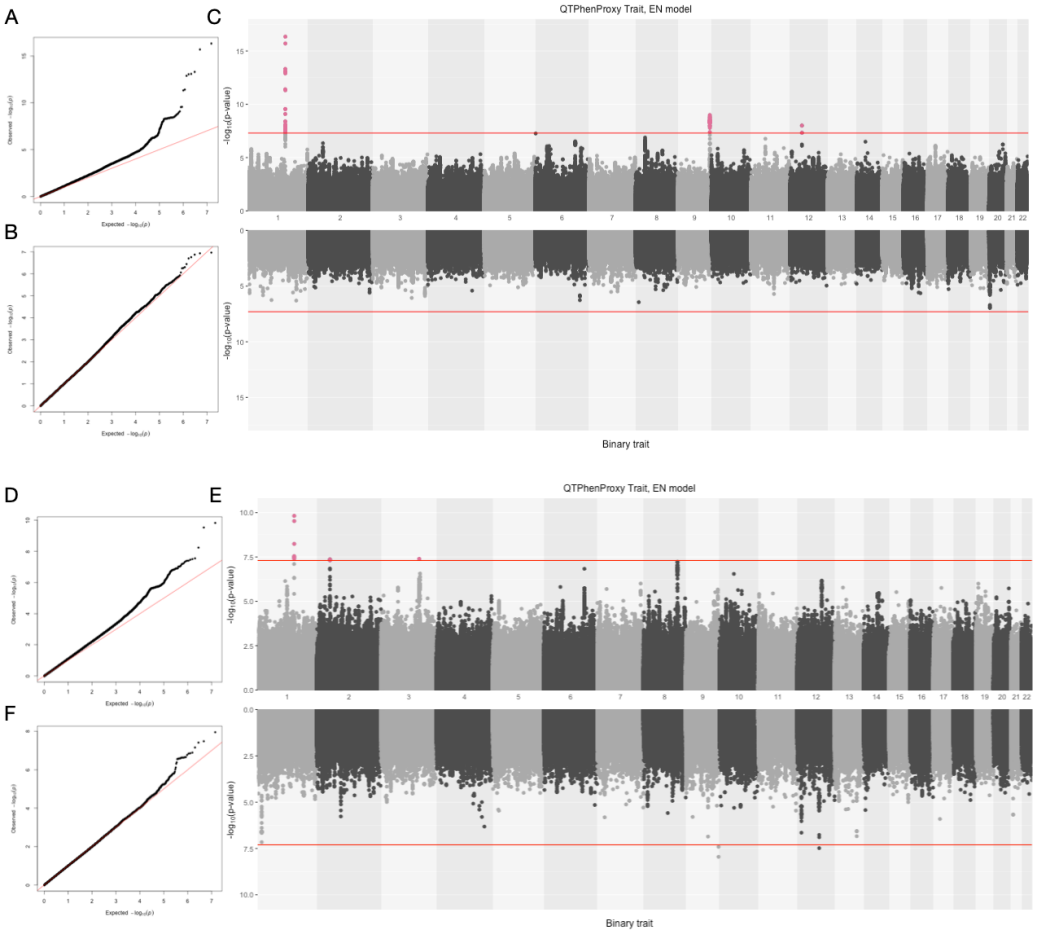

Figure A.4: **QQ Plots and Hudson plot of QTPhenProxy genome-wide association analysis, EN Model with Binary trait genome-wide association analysis for Intracerebral Hemorrhage, (Top) using QC1 quality control and (Bottom) using QC2 quality control, related to Figure 2.** A. and D. Q-Q Plot for QTPhenProxy, EN Model GWAS. B.and E. Q-Q Plot for Binary trait GWAS. C. and F. Top manhattan plot is for QTPhenProxy, bottom plot for binary trait.Variants with p-value $<$ 5e-08 are highlighted in pink, and the dashed lines are at the same value.

bioRxiv preprint doi: https://doi.org/10.1101/2020.01.22.915397; this version posted January 23, 2020. The copyright holder for this preprint (which was not certified by peer review) is the author/funder, who has granted bioRxiv a license to display the preprint in perpetuity. It is made available under aCC-BY 4.0 International license.

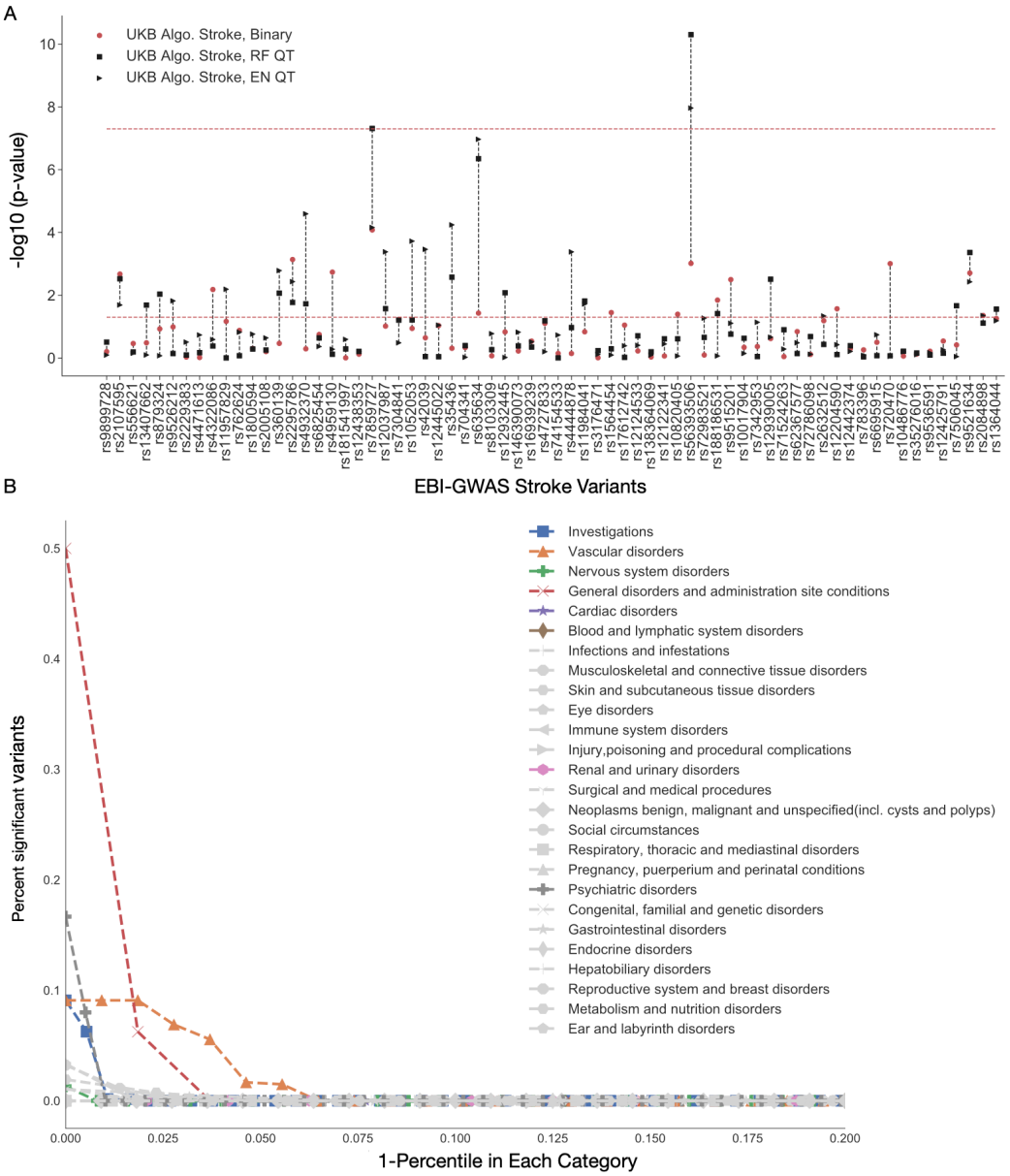

Figure A.5: **QTPhenProxy recovers known stroke variants and variants specific to related organ systems, related to Figure 3.** Results from QTPhenProxy GWAS with QC2 quality control. (A) Horizontal axis shows Stroke variants catalogued in EBI-GWAS that have shown genome-wide significance in previous studies. Black markers represent p-values of variants recovered by QTPhenProxy models (square=RF,Triangle=EN). (B) X-axis is the top percentile of marker sets in each category, Y-axis is the proportion of variants in marker sets that overlap with QTPhenProxy genome-wide significant variants. Each shape corresponds to a disease category. In color are top disease categories: Square=Investigations, Triangle=Vascular disorders, Cross=Nervous system disorders, X=General disorders and administration site conditions, Star=cardiac disorders, and Diamond=Blood and lymphatic system disorders.

bioRxiv preprint doi: https://doi.org/10.1101/2020.01.22.915397; this version posted January 23, 2020. The copyright holder for this preprint (which was not certified by peer review) is the author/funder, who has granted bioRxiv a license to display the preprint in perpetuity. It is made available under aCC-BY 4.0 International license.

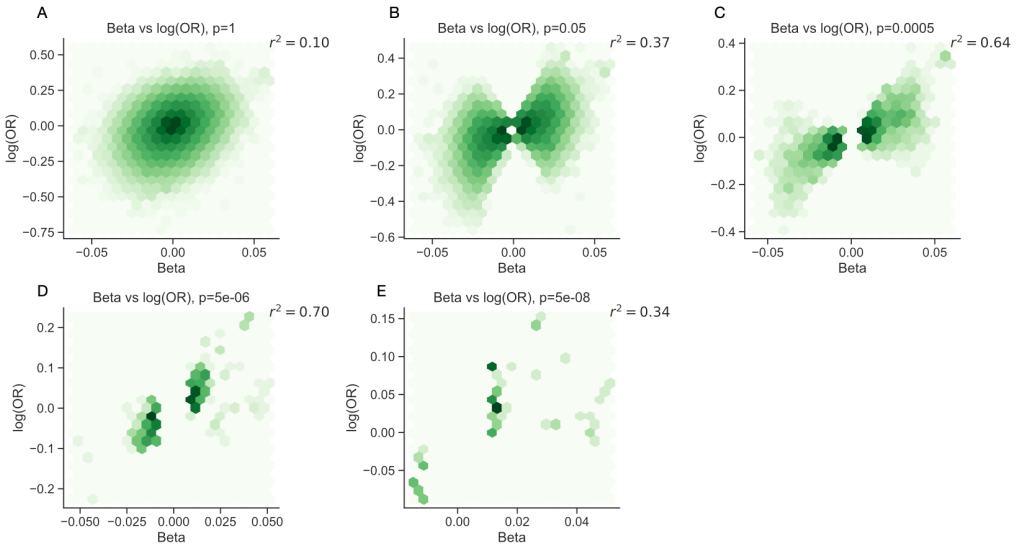

Figure A.6: **Correlation between beta and odds ratio effect sizes for variants at varying degrees of significance, related to Figure 4.** (A-E) Correlation between QTPhenProxy, EN Model for Stroke GWAS and Binary trait GWAS effect size, QC1 quality control. X-axis is QTPhenProxy GWAS beta-coefficients, Y-axis is log base 10 of the Binary GWAS odds ratios. Pearson correlation is recorded in top right corner. From left to right, top to bottom, variants included decreases by restricting p-value.

bioRxiv preprint doi: https://doi.org/10.1101/2020.01.22.915397; this version posted January 23, 2020. The copyright holder for this preprint (which was not certified by peer review) is the author/funder, who has granted bioRxiv a license to display the preprint in perpetuity. It is made available under aCC-BY 4.0 International license.

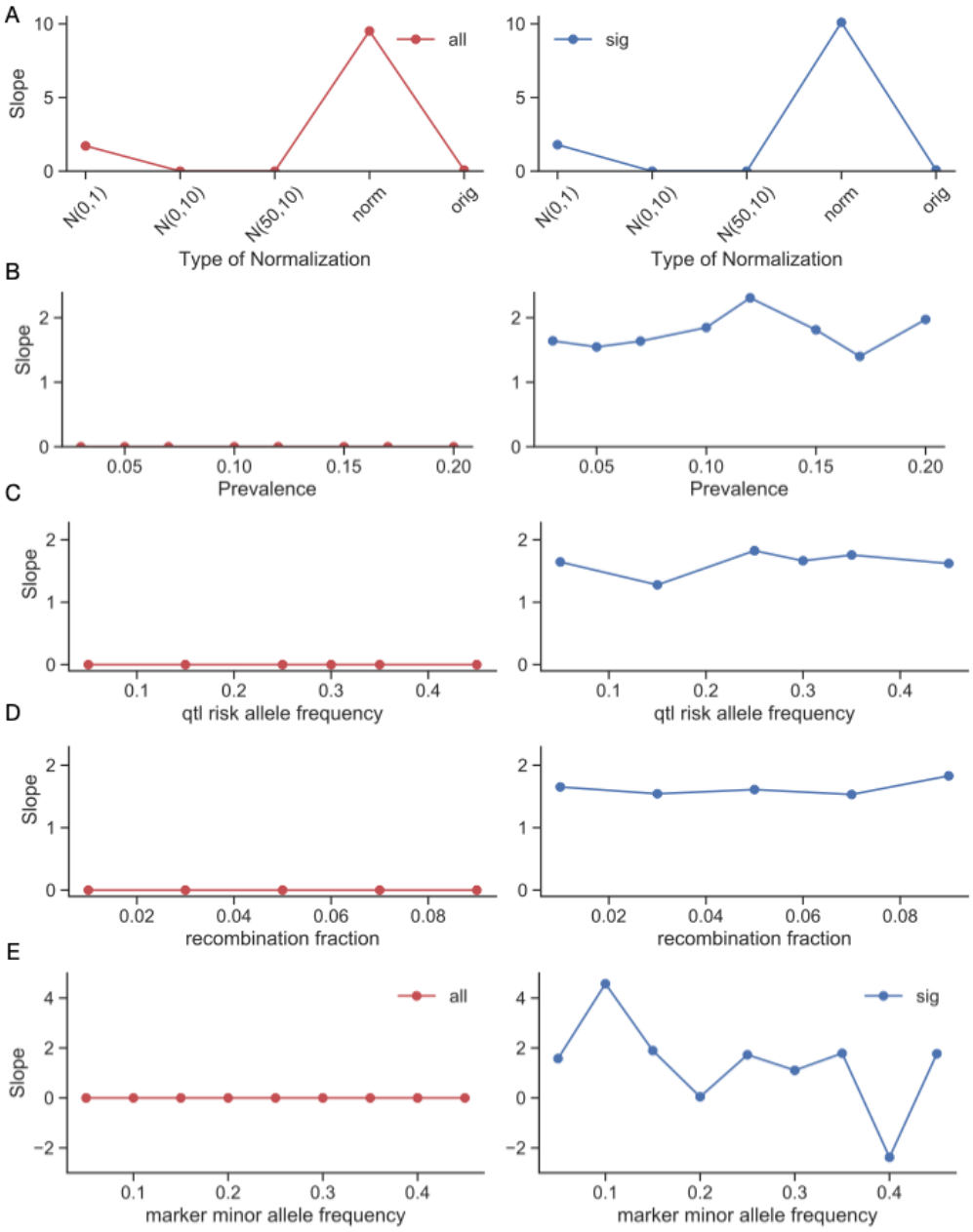

Figure A.7: **Slope of correlation between beta from simulated quantitative trait and log(odds ratio) of simulated binary trait with varying simulation parameters.** Left panels calculate slope with all variants, right panels calculate slope with variants with p-value <0.005. (A) varies the transformation of the probability distribution, where *N(0,1)* is a normal distribution with mean 0, variance 1, *N(0,10)* is a normal distribution with mean 0, variance 10,*N(10,50)* is a normal distribution with mean 10, variance 50, *norm* is normalized by the maximum value, and *orig* is the original distribution. (B) varies the prevalence of the trait, (C) varies the causal allele frequency, (D) varies the recombination fraction between the causal allele and marker allele, and (E) varies the marker minor allele frequency.

bioRxiv preprint doi: https://doi.org/10.1101/2020.01.22.915397; this version posted January 23, 2020. The copyright holder for this preprint (which was not certified by peer review) is the author/funder, who has granted bioRxiv a license to display the preprint in perpetuity. It is made available under aCC-BY 4.0 International license.

Appendix B. Supplementary Tables

Disease	Model	AUROC	AUPRC	Maximum F1
Ischemic Stroke	rf	0.953(0.000279)	0.248(0.00201)	0.326(0.00229)
	ab	0.950(0.000504)	0.246(0.00465)	0.316(0.00335)
	lr	0.946(0.000409)	0.239(0.0021)	0.322(0.00196)
	gb	0.952(0.000686)	0.210(0.00479)	0.294(0.00319)
	en	0.943(0.000362)	0.209(0.00193)	0.295(0.00199)
SAH Stroke	rf	0.875(0.000746)	0.144(0.00299)	0.242(0.00423)
	ab	0.859(0.00186)	0.171(0.0062)	0.271(0.00807)
	lr	0.850(0.00115)	0.151(0.00419)	0.291(0.00509)
	gb	0.863(0.00149)	0.113(0.00379)	0.203(0.00513)
	en	0.863(0.000958)	0.109(0.00377)	0.198(0.00497)
ICH Stroke	rf	0.903(0.000924)	0.0483(0.00143)	0.116(0.00253)
	ab	0.900(0.00171)	0.0480(0.00196)	0.114(0.00305)
	lr	0.879(0.00145)	0.0270(0.000709)	0.0762(0.00137)
	gb	0.900(0.00123)	0.0365(0.00125)	0.0935(0.00227)
	en	0.903(0.00118)	0.0329(0.000755)	0.0861(0.00146)
Stroke	rf	0.899(0.000404)	0.326(0.0016)	0.375(0.00147)
	ab	0.906(0.000711)	0.335(0.00423)	0.380(0.00262)
	lr	0.905(0.000528)	0.314(0.00143)	0.368(0.00154)
	gb	0.903(0.00047)	0.292(0.00245)	0.355(0.00151)
	en	0.896(0.000448)	0.282(0.00113)	0.350(0.000962)

bioRxiv preprint doi: https://doi.org/10.1101/2020.01.22.915397; this version posted January 23, 2020. The copyright holder for this preprint (which was not certified by peer review) is the author/funder, who has granted bioRxiv a license to display the preprint in perpetuity. It is made available under aCC-BY 4.0 International license.

Table B.1: **Phenotyping Models Performance.** *rf*: Random Forest, *ab*= Adaboost, *lr*=Logistic regression with L1 penalty, *gb*=Gradient Boosting, *en*=Logistic Regression with elastic net penalty models. *AUROC*: Area under the Receiver Operating Curve, *AUPRC*: Area under Precision-Recall curve. 95% confidence intervals shown in parentheses

Disease	Model	Prec at 50	Prec at 100	Prec at 500	Prec at N
IscStroke	rf	0.739(0.0132)	0.682(0.0105)	0.544(0.00575)	0.322(0.00246)
	ab	0.71(0.0192)	0.674(0.0154)	0.527(0.0117)	0.309(0.00405)
	lr	0.801(0.0143)	0.672(0.00997)	0.483(0.00560)	0.314(0.00205)
	gb	0.609(0.0305)	0.544(0.0246)	0.425(0.0179)	0.282(0.00714)
	en	0.74(0.0141)	0.63(0.00946)	0.435(0.00476)	0.29(0.00197)
SAHStroke	rf	0.607(0.0178)	0.55(0.0106)	0.308(0.00623)	0.235(0.00381)
	ab	0.627(0.0185)	0.538(0.0144)	0.329(0.0102)	0.266(0.00801)
	lr	0.535(0.0187)	0.5(0.0147)	0.356(0.00722)	0.271(0.00630)
	gb	0.532(0.0203)	0.442(0.0176)	0.249(0.00759)	0.197(0.00557)
	en	0.543(0.0188)	0.441(0.0136)	0.244(0.00773)	0.192(0.00523)
ICHStroke	rf	0.263(0.013)	0.216(0.00968)	0.124(0.00328)	0.110(0.00265)
	ab	0.203(0.0185)	0.171(0.0124)	0.108(0.00400)	0.0997(0.00352)
	lr	0.109(0.0121)	0.100(0.00713)	0.0742(0.00252)	0.0677(0.0027)
	gb	0.137(0.0146)	0.123(0.00838)	0.0908(0.00279)	0.0834(0.00240)
	en	0.123(0.0110)	0.115(0.00761)	0.0835(0.00262)	0.0768(0.00204)
Stroke	rf	0.974(0.00548)	0.941(0.00506)	0.822(0.00339)	0.374(0.0015)
	ab	0.940(0.0120)	0.910(0.0120)	0.813(0.0131)	0.378(0.00265)

bioRxiv preprint doi: https://doi.org/10.1101/2020.01.22.915397; this version posted January 23, 2020. The copyright holder for this preprint (which was not certified by peer review) is the author/funder, who has granted bioRxiv a license to display the preprint in perpetuity. It is made available under aCC-BY 4.0 International license.

lr	0.929(0.00793)	0.872(0.00678)	0.775(0.00413)	0.365(0.00164)
gb	0.868(0.0324)	0.818(0.0309)	0.696(0.0180)	0.351(0.00166)
en	0.848(0.00829)	0.836(0.00706)	0.694(0.00394)	0.345(0.000996)

Table B.2: **Precision at top 50, 100, 500, and N cases probabilities of phenotyping models.** *rf*: Random Forest, *ab*= Adaboost, *lr*=Logistic regression with L1 penalty, *gb*=Gradient Boosting, *en*=Logistic Regression with elastic net penalty models. *Prec*: Precision. 95% confidence intervals

Disease	Model	Sensitivity	Specificity	PPV	NPV
	rf	0.347(0.00483)	0.996(0.000133)	0.00185(2.58e-05)	0.997(2.52e-05)
	ab	0.369(0.00744)	0.995(0.000256)	0.00196(3.99e-05)	0.997(3.86e-05)
Ischemic Stroke	lr	0.362(0.00528)	0.995(0.000127)	0.00192(2.82e-05)	0.997(2.76e-05)
	gb	0.368(0.00868)	0.994(0.000354)	0.00196(4.67e-05)	0.997(4.50e-05)
	en	0.332(0.00624)	0.995(0.000195)	0.00177(3.35e-05)	0.996(3.24e-05)
	rf	0.215(0.00503)	0.999(5.47e-05)	0.000354(8.28e-06)	0.999(8.21e-06)
	ab	0.272(0.00924)	0.999(7.14e-05)	0.000447(1.52e-05)	0.999(1.51e-05)
SAH Stroke	lr	0.266(0.00764)	0.999(6.34e-05)	0.000437(1.26e-05)	0.999(1.25e-05)
	gb	0.204(0.00598)	0.999(9.43e-05)	0.000336(9.86e-06)	0.999(9.75e-06)
	en	0.201(0.00597)	0.999(0.000126)	0.000330(9.85e-06)	0.999(9.68e-06)
	rf	0.133(0.00715)	0.998(0.000140)	0.000174(9.40e-06)	0.999(9.22e-06)
	ab	0.167(0.0113)	0.998(0.000219)	0.000220(1.49e-05)	0.999(1.47e-05)
ICH Stroke	lr	0.177(0.0211)	0.995(0.000742)	0.000233(2.79e-05)	0.999(2.69e-05)
	gb	0.141(0.00950)	0.998(0.000268)	0.000185(1.25e-05)	0.999(1.22e-05)

bioRxiv preprint doi: https://doi.org/10.1101/2020.01.22.915397; this version posted January 23, 2020. The copyright holder for this preprint (which was not certified by peer review) is the author/funder, who has granted bioRxiv a license to display the preprint in perpetuity. It is made available under aCC-BY 4.0 International license.

	en	0.146(0.0123)	0.997(0.000398)	0.000192(1.62e-05)	0.999(1.57e-05)
Stroke	rf	0.377(0.00414)	0.989(0.000286)	0.00648(7.24e-05)	0.989(6.74e-05)
	ab	0.390(0.00559)	0.989(0.000379)	0.00671(9.76e-05)	0.990(9.17e-05)
	lr	0.399(0.00499)	0.987(0.000408)	0.00688(8.81e-05)	0.990(8.1e-05)
	gb	0.388(0.00462)	0.986(0.000373)	0.00670(8.15e-05)	0.989(7.51e-05)
	en	0.393(0.00425)	0.985(0.000336)	0.00678(7.51e-05)	0.990(6.90e-05)

Table B.3: **Sensitivity, Specificity, Positive Predictive Value, and Negative Predictive Value of phenotyping models.** *rf*: Random Forest, *ab*= Adaboost, *lr*=Logistic regression with L1 penalty, *gb*=Gradient Boosting, *en*=Logistic Regression with elastic net penalty models. *PPV*: Positive Predictive Value, *NPV*: Negative Predictive Value. 95% confidence intervals shown in parentheses

Appendix C. Methods

Appendix C.1. QTPhenProxy Phenotyping Model.

We gathered clinical features of primary ICD10 dignosis codes, OCPS4 procedure codes (UK Biobank code 42100), medications (UK Biobank code 20003), race/ethnicity (UK Biobank code 1001), and age. 2018 served as the age end point. We mapped the OCPS4 procedure codes (UK Biobank code 240) to SNOMED-CT codes and the UK Biobank medication codes to RxNorm codes by name National Library of Medicine (b,a). We also gathered data of self reported and first occurrence of all stroke, ischemic stroke, sub-arachnoid stroke, and intracerebral hemorrhage. We made a large matrix in which each extracted EHR feature was a binary variable based on the presence or absence of the feature. We dichotomized

bioRxiv preprint doi: https://doi.org/10.1101/2020.01.22.915397; this version posted January 23, 2020. The copyright holder for this preprint (which was not certified by peer review) is the author/funder, who has granted bioRxiv a license to display the preprint in perpetuity. It is made available under aCC-BY 4.0 International license.

age as greater than or equal or less than 50 years. For each disease, we then defined the cases from the ICD10 code combinations described in the UK Biobank's phenotyping algorithm National Library of Medicine (b). We then trained 5 different classifiers: 1) logistic regression with elastic net penalty, 2) logistic regression with L1 penalty, 3) random forest, 4) adaboost, 5) gradient boosting classifiers on 50% of the cases and an equal number of controls. Controls were identified as subjects without any ICD10 codes within the same category as the Clinical Modification Clinical Classifications Software tool Healthcare Cost and Utilization Project. We then applied the trained algorithm to the whole UK Biobank, resulting in a model probability or quantitative trait proxy for each subject and each disease. For comparison, another phenotype file with binary assignment of case and control for each disease was prepared as well. Table 1 shows the number of cases available for each disease.

Appendix C.2. Evaluation of QTPhenProxy Model Performance.

To evaluate the performance of the QTPhenProxy model, we determined its ability to recover cases when the defining ICD10 codes are removed. We trained 50% of the cases and an equal number of controls on the clinical features described above using the EN and RF classifiers. We chose these classifiers because of their overall high performance and their probability assignment distributions were continuous (Figure 1, Supplementary Figure A.1). We removed the ICD10 codes used to define the cases and controls in our feature set. We then tested the model on all other subjects in the UK Biobank, which included known cases and self-reported cases that did not have an ICD10 code for the disease. We then evaluated the recovery of 1) cross-validation and 2) the holdout test set through Precision at top 50, 100, 500, and number of cases, area under the receiver operating curve,

bioRxiv preprint doi: https://doi.org/10.1101/2020.01.22.915397; this version posted January 23, 2020. The copyright holder for this preprint (which was not certified by peer review) is the author/funder, who has granted bioRxiv a license to display the preprint in perpetuity. It is made available under aCC-BY 4.0 International license.

area under the precision recall curve, and maximum F1 score.

Appendix C.3. Genotyping and Imputation.

UK Biobank subjects that were of White British descent, in the UK Biobank PCA calculations and therefore without 3rd degree and above relatedness, and without aneuploidy were used in this study, totalling 337147 subjects (181,032 females and 156,115 males) Biobank; Bycroft et al. (2018). Of the nearly 500,000 participants, approximately 50,000 subjects were genotyped on the UK BiLEVE Array by Affymetrix while the rest were genotyped using the Applied Biosystems UK Biobank Axiom Array, with over 800,000 markers. The arrays share 95% marker coverage. Initially, we ran a QC extracting markers with an MAF>0.5%, INFO score > 0.3, and hardy-weinberg equilibrium test mid-p value $> 10^{-10}$ using all subjects, which we will refer to as QC1. QC1 was run for GWAS of all 18 diseases. We then re-ran the QC, which we will refer to as QC2, more stringently by extracting markers with an MAF>1%, INFO score > 0.8, and hardy-weinberg equilibrium test mid-p value $> 10^{-5}$ using Plink2 Chang et al. (2015). UKBB version 3 Imputation combined the Haplotype Research Consortium with the UK10K haplotype resource using the software IMPUTE4 Biobank.

Appendix C.4. Genome-wide Association Analysis.

The binary trait and QTPhenProxy probabilities were compared by running two separate association analyses. For both analyses, covariates included age at 2018, sex, first 10 principal components, and the genotyping array the sample was carried out on. In QC1, the original PCs determined by the UKBiobank QC were used. In QC2, we calculated the PCs using the method described in Appendix C.11. QC2 GWAS was only run for stroke, ischemic stroke, subarachnoid

bioRxiv preprint doi: https://doi.org/10.1101/2020.01.22.915397; this version posted January 23, 2020. The copyright holder for this preprint (which was not certified by peer review) is the author/funder, who has granted bioRxiv a license to display the preprint in perpetuity. It is made available under aCC-BY 4.0 International license.

hemorhage, and intracerebral hemorrhage GWAS. For the binary trait GWAS, a logistic regression was run adjusted with the aformentioned covariates. For comparison, the QTPhenProxy probabilities were quantile normalized and run under a linear regression adjusting for the same covariates. We also permuted the probabilities within the phenotyping files and ran additional GWAS 10 times to ensure the signal was correlated with the phenotype.

Appendix C.5. Mapping variants to known disease variant marker sets and mapping marker sets to disease systems.

The EBI-GWAS catalogue has a database of all published GWAS Buniello et al. (2019). We extracted over 2,000 disease marker sets conducted on populations with European ancestry. MedDRA is a standardized medical vocabulary developed by International Council for Harmonisation of Technical Requirements for Pharmaceuticals for Human Use (ICH) Brown (1999). All terms in the vocabulary can be mapped to its highest system level, which includes 27 different organ systems and other general and lab studies such as social circumstance and investigations. Using the NCBO annotator, we mapped the names of the EBI-GWAS disease marker sets to the MedDRA System Organ Classes level Whetzel et al. (2011).

Appendix C.6. Assessing the specificity of the QTPhenProxy-derived variants.

To assess the disease specificity of the genome-wide significant variants, we first calculated the proportion of genome-wide significant variants in each of the EBI-GWAS disease marker sets. We then aggregated the marker sets together by System Organ Class to evaluate the systems enriched for genome-wide significant variants. We ordered the marker sets in each class by proportion of genome-wide significant variants and divided by the number of marker sets in each class. We

bioRxiv preprint doi: https://doi.org/10.1101/2020.01.22.915397; this version posted January 23, 2020. The copyright holder for this preprint (which was not certified by peer review) is the author/funder, who has granted bioRxiv a license to display the preprint in perpetuity. It is made available under aCC-BY 4.0 International license.

also compared the proportion of variants of varying significance of the marker sets related to each disease with 1) the other marker sets related to the same System Organ Class as the disease and 2) all other marker sets. We stratified each comparison by significance value, between 0.05 and 5E-08.

Appendix C.7. Evaluation of recovery of known variants

For each disease, we gathered EBI-GWAS marker sets that contained the disease in its name. These represent known variants of each disease. We then extracted the p-value from either the binary trait logistic regression or QTPhenProxy linear regression. We then ran a t-test comparing the negative log base 10 p-values of the binary trait with QTPhenProxy GWAS. We also ran a t-test comparing the difference between the binary and QTPhenProxy log base 10 p values for the known ischemic stroke variants and an equivalent number of random variants.

Appendix C.8. Refinement of discovered variants by QTPhenProxy using conditional analysis

At each LD-independent locus, the SNP with lowest p-value may not be the variant that causes the most phenotypic variation within the area Yang et al. (2012). Therefore, we applied GCTA-COJO, a conditional analysis that takes into account lead SNPs and the LD structure of a sample of the population, to our genome-wide association results Yang et al. (2012). We randomly sampled 10,000 subjects from the UKBiobank for the linkage disequilibrium calculation Wells et al. (2019). From the GCTA-COJO results, we then mapped each locus to its nearest gene using dbSNP and the UCSC Genome Browser accessed at http://genome.ucsc.edu/ National Center for Biotechnology Information, National Library of Medicine.;

bioRxiv preprint doi: https://doi.org/10.1101/2020.01.22.915397; this version posted January 23, 2020. The copyright holder for this preprint (which was not certified by peer review) is the author/funder, who has granted bioRxiv a license to display the preprint in perpetuity. It is made available under aCC-BY 4.0 International license.

Kent et al. (2002). For intergenic loci, we chose the 1-2 nearest genes that were at most 10,000 KB away.

Appendix C.9. Correlation of QTPhenProxy GWAS beta coefficients to Binary trait GWAS Odds Ratio

We calculated the Pearson correlation between the beta-coefficients of the QTPhenProxy GWAS and log of the odds ratios of the Binary trait GWAS. In order to account for noise, we calculated the correlation with variants with different levels of significance in the QTPhenProxy models. P-value cutoffs included 1, 0.05,0.0005,5e-06,and 5e-08.

Appendix C.10. Simulation of Conversion of QTPhenProxy trait to Binary trait and Conversion of beta coefficients to odds ratios

Based on the scale difference between binary and quantitative traits, the odds ratios are not directly comparable. We decided to simulate a method to convert beta coefficients from QTPhenProxy to Odds ratios. We did this by simulating a quantitative trait, converting it to a binary trait, and testing the correlation of a simulated marker variant's significance between the two methods. Using SOLAR, a software package for estimating heritability using identity by descent calculations, we simulated a quantitative trait with one quantitative trait locus with two alleles and a nearby marker locus with two alleles Almasy and Blangero (1998). We first removed all related individuals with a resulting cohort of 4,195 subjects. For the simulation, we varied the frequency for the causal minor allele and a marker minor allele from 0.05-0.45 in increments of 0.010, the mean quantitative trait value for the heterozygous genotype from 5-45 in increments of 10 and the homozygous genotypes' $mean \pm 50$, the standard deviation of the

bioRxiv preprint doi: https://doi.org/10.1101/2020.01.22.915397; this version posted January 23, 2020. The copyright holder for this preprint (which was not certified by peer review) is the author/funder, who has granted bioRxiv a license to display the preprint in perpetuity. It is made available under aCC-BY 4.0 International license.

quantitative trait from 5-20 in increments of 4, and the recombinant fraction from 0.01-0.10 in increments of 0.02. After simulating the quantitative trait distribution, we then normalized the trait to several distributions: standard normal, normal distribution with mean 0 and standard deviation 10, and mean 50 and standard deviation 10. We compared distributions because we quantile normalized our QTPhenProxy trait values before running the genome-wide associations studies. We then converted each simulation to a binary trait using liability thresholding Risch (1990). Liability thresholding was implemented as follows: We determined a quantitative trait value as a threshold based off the prevalence of the simulated trait, which we varied from 2.5-20% in increments of 5%. Any subjects above this threshold is labeled a case, and the rest controls in the binary trait phenotype. We then ran linear or logistic regressions using the python package statsmodels between the simulated quantitative trait or the binary trait and the subjects'genotypes for the marker and causal loci National Library of Medicine (b). We developed a conversion formula for the beta coefficients to odds ratios by linearly regressing the correlation between the simulated effect sizes. We then converted the beta-coefficients to odds ratios of the UK Biobank GWAS results by multiplying the beta coefficient by the average slope and intercept and then taking the exponential of the result.

Appendix C.11. PCA

In order to confirm the cases were well distributed within the data and to determine the number of principal components to use as covariates, we conducted PCA. For each of the four diseases, we first pruned the variants used for PCA by running a sliding window of size 100 kbps, 5 variant step size, and r^2 threshold of 0.1. We then combined the chromosomes, extracting only the pruned variants,

bioRxiv preprint doi: https://doi.org/10.1101/2020.01.22.915397; this version posted January 23, 2020. The copyright holder for this preprint (which was not certified by peer review) is the author/funder, who has granted bioRxiv a license to display the preprint in perpetuity. It is made available under aCC-BY 4.0 International license.

using plink2 and cat-bgen software Band and Marchini (2018). We then ran pca with plink2 Chang et al. (2015) and evaluated the PCs to be used as covariates using a skree plot. Within the main PCs, we plotted them against each other, highlighting the distribution of the cases.

Appendix C.12. LD Score Regression and evaluation of genomic inflation

We determined the lambda genomic correction and LD score regression coefficient using the software LDSC Bulik-Sullivan et al. (2015). We used the disease GWAS summary statistics and European LD scores pre-computed from 1000 genomes by the Alkes group Bulik-Sullivan et al. (2015). QQ plots were plotted using qqman Turner (2014). To determine the relationship between genomic inflation and minor allele frequency, we binned all variants in the stroke gwas by minor allele frequency into 30 bins. We then calculated the genomic inflation of the p-values of the variants in each bin.

Appendix C.13. Data and Code Availability Statements

The EBI-GWAS marker set- MedDRA mappings and code generated in this study will be made publicly available online at https://github.com/pthangaraj/QTPhenProxy in February 2020. Currently, it is available upon request.

References

Abraham, G., Malik, R., Yonova-Doing, E., Salim, A., Wang, T., Danesh, J., Butterworth, A.S., Howson, J.M.M., Inouye, M., Dichgans, M., 2019. Genomic risk score offers predictive performance comparable to clinical risk factors for ischaemic stroke. Nature Communications 10,

bioRxiv preprint doi: https://doi.org/10.1101/2020.01.22.915397; this version posted January 23, 2020. The copyright holder for this preprint (which was not certified by peer review) is the author/funder, who has granted bioRxiv a license to display the preprint in perpetuity. It is made available under aCC-BY 4.0 International license.

5819. URL: http://www.nature.com/articles/s41467-019-13848-1, doi:10.1038/s41467-019-13848-1.

Almasy, L., Blangero, J., 1998. Multipoint Quantitative-Trait Linkage Analysis in General Pedigrees. The American Journal of Human Genetics 62, 1198–1211. URL: https://linkinghub.elsevier.com/retrieve/pii/S0002929707615420, doi:10.1086/301844.

Asselta, R., Peyvandi, F., 2009. Factor V deficiency. Seminars in Thrombosis and Hemostasis 35, 382–389. doi:10.1055/s-0029-1225760.

Band, G., Marchini, J., 2018. BGEN: a binary file format for imputed genotype and haplotype data. bioRxiv , 308296URL: https://www.biorxiv.org/content/10.1101/308296v2, doi:10.1101/308296.

Biobank, U., . Genotyping and quality control of UK Biobank, a large-scale, extensively phenotyped prospective resource. URL: http://www.ukbiobank.ac.uk/wp-content/uploads/2014/04/UKBiobank$_{g}enotyping_{Q}C_{d}ocumentation-web.pdf.Brown, E.,$ 1999$.CodingofDataMedDRAandotherMedicalTechnologies, in:ClinicalDataManagement.Chichester, UK, p.$177. URL:$ 10.1002/0470846364.ch10.

Brown, M.S., Goldstein, J.L., 1979. Receptor-mediated endocytosis: insights from the lipoprotein receptor system. Proceedings of the National Academy of Sciences of the United States of America 76, 3330–3337.

bioRxiv preprint doi: https://doi.org/10.1101/2020.01.22.915397; this version posted January 23, 2020. The copyright holder for this preprint (which was not certified by peer review) is the author/funder, who has granted bioRxiv a license to display the preprint in perpetuity. It is made available under aCC-BY 4.0 International license.

Bulik-Sullivan, B.K., Loh, P.R., Finucane, H.K., Ripke, S., Yang, J., Patterson, N., Daly, M.J., Price, A.L., Neale, B.M., 2015. LD Score regression distinguishes confounding from polygenicity in genome-wide association studies. Nature Genetics 47, 291–295. URL: https://www.nature.com/articles/ng.3211, doi:10.1038/ng.3211.

Buniello, A., MacArthur, J.A.L., Cerezo, M., Harris, L.W., Hayhurst, J., Malangone, C., McMahon, A., Morales, J., Mountjoy, E., Sollis, E., Suveges, D., Vrousgou, O., Whetzel, P.L., Amode, R., Guillen, J.A., Riat, H.S., Trevanion, S.J., Hall, P., Junkins, H., Flicek, P., Burdett, T., Hindorff, L.A., Cunningham, F., Parkinson, H., 2019. The NHGRI-EBI GWAS Catalog of published genome-wide association studies, targeted arrays and summary statistics 2019. Nucleic Acids Research 47, D1005–D1012. URL: https://academic.oup.com/nar/article/47/D1/D1005/5184712, doi:10.1093/nar/gky1120.

Bycroft, C., Freeman, C., Petkova, D., Band, G., Elliott, L.T., Sharp, K., Motyer, A., Vukcevic, D., Delaneau, O., O' Connell, J., Cortes, A., Welsh, S., Young, A., Effingham, M., McVean, G., Leslie, S., Allen, N., Donnelly, P., Marchini, J., 2018. The UK Biobank resource with deep phenotyping and genomic data. Nature 562, 203–209. URL: http://www.nature.com/articles/s41586-018-0579-z, doi:10.1038/s41586-018-0579-z.

Chang, C.C., Chow, C.C., Tellier, L.C., Vattikuti, S., Purcell, S.M., Lee, J.J., 2015. Second-generation PLINK: rising to the challenge of larger and richer datasets. GigaScience 4, 7. URL:

bioRxiv preprint doi: https://doi.org/10.1101/2020.01.22.915397; this version posted January 23, 2020. The copyright holder for this preprint (which was not certified by peer review) is the author/funder, who has granted bioRxiv a license to display the preprint in perpetuity. It is made available under aCC-BY 4.0 International license.

https://academic.oup.com/gigascience/article-lookup/doi/10.1186/s13742-015-0047-8, doi:10.1186/s13742-015-0047-8.

DeBoever, C., Tanigawa, Y., Aguirre, M., McInnes, G., Lavertu, A., Rivas, M.A., 2019. Assessing digital phenotyping to enhance genetic studies of human diseases. preprint. Genetics. URL: http://biorxiv.org/lookup/doi/10.1101/738856, doi:10.1101/738856.

Erdmann, J., Grosshennig, A., Braund, P.S., Konig, I.R., Hengstenberg, C., Hall, A.S., Linsel-Nitschke, P., Kathiresan, S., Wright, B., Tregouet, D.A., Cambien, F., Bruse, P., Aherrahrou, Z., Wagner, A.K., Stark, K., Schwartz, S.M., Salomaa, V., Elosua, R., Melander, O., Voight, B.F., O' Donnell, C.J., Peltonen, L., Siscovick, D.S., Altshuler, D., Merlini, P.A., Peyvandi, F., Bernardinelli, L., Ardissino, D., Schillert, A., Blankenberg, S., Zeller, T., Wild, P., Schwarz, D.F., Tiret, L., Perret, C., Schreiber, S., El Mokhtari, N.E., Schafer, A., Marz, W., Renner, W., Bugert, P., KlÃŒter, H., Schrezenmeir, J., Rubin, D., Ball, S.G., Balmforth, A.J., Wichmann, H.E., Meitinger, T., Fischer, M., Meisinger, C., Baumert, J., Peters, A., Ouwehand, W.H., Italian Atherosclerosis, Thrombosis, and Vascular Biology Working Group, Myocardial Infarction Genetics Consortium, Wellcome Trust Case Control Consortium, Cardiogenics Consortium, Deloukas, P., Thompson, J.R., Ziegler, A., Samani, N.J., Schunkert, H., 2009. New susceptibility locus for coronary artery disease on chromosome 3q22.3. Nature Genetics 41, 280–282.

Erqou, S., Thompson, A., Angelantonio, E.D., Saleheen, D., Kaptoge, S., Marcovina, S., Danesh, J., 2010. Apolipoprotein(a) Isoforms and the Risk

bioRxiv preprint doi: https://doi.org/10.1101/2020.01.22.915397; this version posted January 23, 2020. The copyright holder for this preprint (which was not certified by peer review) is the author/funder, who has granted bioRxiv a license to display the preprint in perpetuity. It is made available under aCC-BY 4.0 International license.

of Vascular Disease: Systematic Review of 40 Studies Involving 58,000 Participants. Journal of the American College of Cardiology 55, 2160–2167. URL: http://www.onlinejacc.org/content/55/19/2160, doi:10.1016/j.jacc.2009.10.080.

Farah, C., Michel, L.Y.M., Balligand, J.L., 2018. Nitric oxide signalling in cardiovascular health and disease. Nature Reviews Cardiology 15, 292–316. URL: https://www.nature.com/articles/nrcardio.2017.224, doi:10.1038/nrcardio.2017.224.

Fessler, M.B., Arndt, P.G., Frasch, S.C., Lieber, J.G., Johnson, C.A., Murphy, R.C., Nick, J.A., Bratton, D.L., Malcolm, K.C., Worthen, G.S., 2004. Lipid Rafts Regulate Lipopolysaccharide-induced Activation of Cdc42 and Inflammatory Functions of the Human Neutrophil. Journal of Biological Chemistry 279, 39989–39998. URL: http://www.jbc.org/lookup/doi/10.1074/jbc.M401080200, doi:10.1074/jbc.M401080200.

Gao Yang, Stuart Deborah, Takahishi Takamune, Kohan Donald E., 2018. NephronâSpecific Disruption of Nitric Oxide Synthase 3 Causes Hypertension and Impaired Salt Excretion. Journal of the American Heart Association 7, e009236. URL: https://www.ahajournals.org/doi/full/10.1161/JAHA.118.009236, doi:10.1161/JAHA.118.009236.

Hashimoto, K., Ochi, H., Sunamura, S., Kosaka, N., Mabuchi, Y., Fukuda, T., Yao, K., Kanda, H., Ae, K., Okawa, A., Akazawa, C., Ochiya, T., Futakuchi, M., Takeda, S., Sato, S., 2018. Cancer-secreted hsa-miR-940 induces an osteoblastic

bioRxiv preprint doi: https://doi.org/10.1101/2020.01.22.915397; this version posted January 23, 2020. The copyright holder for this preprint (which was not certified by peer review) is the author/funder, who has granted bioRxiv a license to display the preprint in perpetuity. It is made available under aCC-BY 4.0 International license.

phenotype in the bone metastatic microenvironment via targeting ARHGAP1 and FAM134a. Proceedings of the National Academy of Sciences 115, 2204–2209. URL: https://www.pnas.org/content/115/9/2204, doi:10.1073/pnas.1717363115.

Healthcare Cost and Utilization Project, . Multi-level procedures ccs categories. https://www.hcup-us.ahrq.gov/toolssoftware/ccs10/ccs10.jspdownload.

Hinds, D.A., Buil, A., Ziemek, D., Martinez-Perez, A., Malik, R., Folkersen, L., Germain, M., Malarstig, A., Brown, A., Soria, J.M., Dichgans, M., Bing, N., Franco-Cereceda, A., Souto, J.C., Dermitzakis, E.T., Hamsten, A., Worrall, B.B., Tung, J.Y., METASTROKE Consortium, INVENT Consortium, Sabater-Lleal, M., 2016. Genome-wide association analysis of self-reported events in 6135 individuals and 252 827 controls identifies 8 loci associated with thrombosis. Human Molecular Genetics 25, 1867–1874. doi:10.1093/hmg/ddw037.

Howrigan, D., Abbott, L., Churchhouse, C., Palmer, D., 2017. UK Biobank. http://www.nealelab.is/uk-biobank.

Jiang, F., Dong, Y., Wu, C., Yang, X., Zhao, L., Guo, J., Li, Y., Dong, J., Zheng, G.Y., Cao, H., Jin, L., Ren, Y., Cheng, W., Li, W., Tian, X.L., Li, X., 2011. Fine mapping of chromosome 3q22.3 identifies two haplotype blocks in ESYT3 associated with coronary artery disease in female Han Chinese. Atherosclerosis 218, 397–403. URL: http://www.sciencedirect.com/science/article/pii/S00219150110049 doi:10.1016/j.atherosclerosis.2011.06.017.

bioRxiv preprint doi: https://doi.org/10.1101/2020.01.22.915397; this version posted January 23, 2020. The copyright holder for this preprint (which was not certified by peer review) is the author/funder, who has granted bioRxiv a license to display the preprint in perpetuity. It is made available under aCC-BY 4.0 International license.

Kent, W.J., Sugnet, C.W., Furey, T.S., Roskin, K.M., Pringle, T.H., Zahler, A.M., Haussler, D., 2002. The Human Genome Browser at UCSC 12, 996–1006.

Kohane, I.S., 2011. Using electronic health records to drive discovery in disease genomics. Nature Reviews Genetics 12, 417–428. URL: http://www.nature.com/articles/nrg2999, doi:10.1038/nrg2999.

Kujovich, J.L., 2011. Factor V Leiden thrombophilia. Genetics in Medicine: Official Journal of the American College of Medical Genetics 13, 1–16. doi:10.1097/GIM.0b013e3181faa0f2.

Ligthart, S., Vaez, A., Hsu, Y.H., Inflammation Working Group of the CHARGE Consortium, PMI-WG-XCP, LifeLines Cohort Study, Stolk, R., Uitterlinden, A.G., Hofman, A., Alizadeh, B.Z., Franco, O.H., Dehghan, A., 2016. Bivariate genome-wide association study identifies novel pleiotropic loci for lipids and inflammation. BMC Genomics 17, 443. URL: http://bmcgenomics.biomedcentral.com/articles/10.1186/s12864-016-2712-4, doi:10.1186/s12864-016-2712-4.

Liu, J.Z., Erlich, Y., Pickrell, J.K., 2017. Caseâcontrol association mapping by proxy using family history of disease. Nature Genetics 49, 325–331. URL: http://www.nature.com/articles/ng.3766, doi:10.1038/ng.3766.

Lucas, A., . hudson: R package. https://github.com/anastasia-lucas/hudson.

Maher, B., 2008. Personal genomes: The case of the missing heritability. Nature 456, 18–21. doi:10.1038/456018a.

bioRxiv preprint doi: https://doi.org/10.1101/2020.01.22.915397; this version posted January 23, 2020. The copyright holder for this preprint (which was not certified by peer review) is the author/funder, who has granted bioRxiv a license to display the preprint in perpetuity. It is made available under aCC-BY 4.0 International license.

Malik, R., Chauhan, G., Traylor, M., Sargurupremraj, M., Okada, Y., Mishra, A., Rutten-Jacobs, L., Giese, A.K., van der Laan, S.W., Gretarsdottir, S., et al., 2018a. Multiancestry genome-wide association study of 520,000 subjects identifies 32 loci associated with stroke and stroke subtypes. Nature Genetics 50, 1–14. doi:10.1038/s41588-018-0058-3.

Malik, R., Rannikmae, K., Traylor, M., Georgakis, M.K., Sargurupremraj, M., Markus, H.S., Hopewell, J.C., Debette, S., Sudlow, C.L.M., Dichgans, M., for the MEGASTROKE consortium and the International Stroke Genetics Consortium, 2018b. Genome-wide meta-analysis identifies 3 novel loci associated with stroke: MEGASTROKE and UK Biobank GWAS. Annals of Neurology 84, 934–939. URL: http://doi.wiley.com/10.1002/ana.25369, doi:10.1002/ana.25369.

McCarthy, M.I., Abecasis, G.R., Cardon, L.R., Goldstein, D.B., Little, J., Ioannidis, J.P.A., Hirschhorn, J.N., 2008. Genome-wide association studies for complex traits: consensus, uncertainty and challenges. Nature Reviews Genetics 9, 356–369. URL: http://www.nature.com/articles/nrg2344, doi:10.1038/nrg2344.

National Center for Biotechnology Information, National Library of Medicine., . Database of single nucleotide polymorphisms (dbsnp). http://www.ncbi.nlm.nih.gov/SNP/. (dbSNP Build ID: GRCh37.p13), Bethesda, MD.

National Library of Medicine, a. UMLS Metathesaurus - RXNORM. URL: https://www.nlm.nih.gov/research/umls/sourcereleasedocs/current/

bioRxiv preprint doi: https://doi.org/10.1101/2020.01.22.915397; this version posted January 23, 2020. The copyright holder for this preprint (which was not certified by peer review) is the author/funder, who has granted bioRxiv a license to display the preprint in perpetuity. It is made available under aCC-BY 4.0 International license.

National Library of Medicine, b. Unified Medical Language System SNOMED CT to ICD-10-CM Map. URL: https://www.nlm.nih.gov/research/umls/mapping$_{p}rojects/snomedct_{t}o_{i}cd10cm$ -228.

Schnier, C., Bush, K., Nolan, J., Sudlow, C.L.M., UK Biobank Outcome Adjuducation Group, 2017. Definitions of Stroke for UK Biobank Phase 1 Outcomes Adjudication. URL: https://biobank.ctsu.ox.ac.uk/crystal/crystal/docs/alg$_{o}utcome_{s}troke.$ $EJPN : officialjournaloftheEuropeanPaediatricNeurologySociety20, 474-$ $-479. doi : 10.1016/j.ejpn.2016.01.002$.

Seabold, S., Perktold, J., 2010. Statsmodels: Econometric and statistical modeling with python, in: 9th Python in Science Conference.

Sinnott, J.A., Cai, F., Yu, S., Hejblum, B.P., Hong, C., Kohane, I.S., Liao, K.P., 2018. PheProb: probabilistic phenotyping using diagnosis codes to improve power for genetic association studies. Journal of the American Medical Informatics Association 25, 1359–1365. URL: https://academic.oup.com/jamia/article/25/10/1359/4999078, doi:10.1093/jamia/ocy056.

Song, Y., Ma, R., Zhang, H., 2019. The influence of MRAS gene variants on ischemic stroke and serum lipid levels in Chinese Han population. Medicine 98, e18065. URL: https://journals.lww.com/md-journal/FullText/2019/11290/The$_{i}nfluence_{o}f_{M}RAS_{g}ene_{v}ariants_{o}n_{i}schemic.32.asp$ $10.1097/MD.0000000000018065. Thangaraj, P.M., Kummer, B.R., Lorberbaum, T., Elkind, M.V$ $basedstrokephenotypingmethods.$ $bioRxivURL$:

bioRxiv preprint doi: https://doi.org/10.1101/2020.01.22.915397; this version posted January 23, 2020. The copyright holder for this preprint (which was not certified by peer review) is the author/funder, who has granted bioRxiv a license to display the preprint in perpetuity. It is made available under aCC-BY 4.0 International license.

https://www.biorxiv.org/content/early/2019/06/22/565671, *doi* : 10.1101/565671.

The Emerging Risk Factors Collaboration, 2009. Lipoprotein(a) Concentration and the Risk of Coronary Heart Disease, Stroke, and Nonvascular Mortality. JAMA : the journal of the American Medical Association 302, 412–423. URL: https://www.ncbi.nlm.nih.gov/pmc/articles/PMC3272390/, doi:10.1001/jama.2009.1063.

Turner, S.D., 2014. qqman: an R package for visualizing GWAS results using Q-Q and manhattan plots. bioRxiv , 005165URL: https://www.biorxiv.org/content/10.1101/005165v1, doi:10.1101/005165.

Wang Long, Chen Juan, Zeng Ying, Wei Jie, Jing Jinjin, Li Ge, Su Li, Tang Xiaojun, Wu Tangchun, Zhou Li, 2016. Functional Variant in the SLC22a3-LPAL2-LPA Gene Cluster Contributes to the Severity of Coronary Artery Disease. Arteriosclerosis, Thrombosis, and Vascular Biology 36, 1989–1996. URL: https://www.ahajournals.org/doi/full/10.1161/ATVBAHA.116.307311, doi:10.1161/ATVBAHA.116.307311.

Weiskopf, N.G., Hripcsak, G., Swaminathan, S., Weng, C., 2013. Defining and measuring completeness of electronic health records for secondary use. Journal of biomedical informatics 46, 830–836.

Wells, H.R., Freidin, M.B., Zainul Abidin, F.N., Payton, A., Dawes, P., Munro, K.J., Morton, C.C., Moore, D.R., Dawson, S.J., Williams, F.M., 2019. GWAS Identifies 44 Independent Associated Genomic

bioRxiv preprint doi: https://doi.org/10.1101/2020.01.22.915397; this version posted January 23, 2020. The copyright holder for this preprint (which was not certified by peer review) is the author/funder, who has granted bioRxiv a license to display the preprint in perpetuity. It is made available under aCC-BY 4.0 International license.

Loci for Self-Reported Adult Hearing Difficulty in UK Biobank. The American Journal of Human Genetics 105, 788–802. URL: https://linkinghub.elsevier.com/retrieve/pii/S0002929719303477, doi:10.1016/j.ajhg.2019.09.008.

Whetzel, P.L., Noy, N.F., Shah, N.H., Alexander, P.R., Nyulas, C., Tudorache, T., Musen, M.A., 2011. BioPortal: enhanced functionality via new Web services from the National Center for Biomedical Ontology to access and use ontologies in software applications. Nucleic Acids Research 39, W541–W545. URL: https://academic.oup.com/nar/article-lookup/doi/10.1093/nar/gkr469, doi:10.1093/nar/gkr469.

Yang, J., Ferreira, T., Morris, A.P., Medland, S.E., Genetic Investigation of ANthropometric Traits (GIANT) Consortium, DIAbetes Genetics Replication And Meta-analysis (DIAGRAM) Consortium, Madden, P.A.F., Heath, A.C., Martin, N.G., Montgomery, G.W., Weedon, M.N., Loos, R.J., Frayling, T.M., McCarthy, M.I., Hirschhorn, J.N., Goddard, M.E., Visscher, P.M., 2012. Conditional and joint multiple-SNP analysis of GWAS summary statistics identifies additional variants influencing complex traits. Nature Genetics 44, 369–375. URL: http://www.nature.com/articles/ng.2213, doi:10.1038/ng.2213.

Yang, J., Wray, N.R., Visscher, P.M., 2009. Comparing apples and oranges: equating the power of case-control and quantitative trait association studies. Genetic Epidemiology , n/a–n/aURL: http://doi.wiley.com/10.1002/gepi.20456, doi:10.1002/gepi.20456.

bioRxiv preprint doi: https://doi.org/10.1101/2020.01.22.915397; this version posted January 23, 2020. The copyright holder for this preprint (which was not certified by peer review) is the author/funder, who has granted bioRxiv a license to display the preprint in perpetuity. It is made available under aCC-BY 4.0 International license.

Zaitlen, N., Pasaniuc, B., Patterson, N., Pollack, S., Voight, B., Groop, L., Altshuler, D., Henderson, B.E., Kolonel, L.N., Marchand, L.L., Waters, K., Haiman, C.A., Stranger, B.E., Dermitzakis, E.T., Kraft, P., Price, A.L., 2012. Analysis of case-control association studies with known risk variants. Bioinformatics 28, 1729–1737. URL: https://academic.oup.com/bioinformatics/article-lookup/doi/10.1093/bioinformatics/bts259, doi:10.1093/bioinformatics/bts259.

Zaykin, D.V., Zhivotovsky, L.A., 2005. Ranks of Genuine Associations in Whole-Genome Scans. Genetics 171, 813–823. URL: http://www.genetics.org/lookup/doi/10.1534/genetics.105.044206, doi:10.1534/genetics.105.044206.

Zhang, X., Guan, J., Guo, M., Dai, H., Cai, S., Zhou, C., Wang, Y., Qin, Q., 2019. Rho GTPaseâactivating protein 1 promotes apoptosis of myocardial cells in an ischemic cardiomyopathy model. Kardiologia Polska 77, 1163–1169. doi:10.33963/KP.15040.

Zheng, P.F., Yin, R.X., Deng, G.X., Guan, Y.Z., Wei, B.L., Liu, C.X., 2019. Association between the XKR6 rs7819412 SNP and serum lipid levels and the risk of coronary artery disease and ischemic stroke. BMC Cardiovascular Disorders 19, 202. URL: https://doi.org/10.1186/s12872-019-1179-z, doi:10.1186/s12872-019-1179-z.

Zhou, W., Nielsen, J.B., Fritsche, L.G., Dey, R., Gabrielsen, M.E., Wolford, B.N., LeFaive, J., VandeHaar, P., Gagliano, S.A., Gifford, A., Bastarache, L.A., Wei, W.Q., Denny, J.C., Lin, M., Hveem, K., Kang, H.M., Abecasis, G.R., Willer, C.J.,

bioRxiv preprint doi: https://doi.org/10.1101/2020.01.22.915397; this version posted January 23, 2020. The copyright holder for this preprint (which was not certified by peer review) is the author/funder, who has granted bioRxiv a license to display the preprint in perpetuity. It is made available under aCC-BY 4.0 International license.

Lee, S., 2018. Efficiently controlling for case-control imbalance and sample relatedness in large-scale genetic association studies. Nature Genetics 50, 1335–1341. URL: https://www.nature.com/articles/s41588-018-0184-y, doi:10.1038/s41588-018-0184-y.